Ecological Monographs, 80(4), 2010, pp. 569–608

High-dimensional coexistence based on individual variation: a synthesis of evidence

James S. Clark,[1,2,3,5] David Bell,[1] Chengjin Chu,[1] Benoit Courbaud,[1] Michael Dietze,[1] Michelle Hersh,[1,2] Janneke HilleRisLambers,[2] Inés Ibáñez,[2] Shannon LaDeau,[4] Sean McMahon,[1] Jessica Metcalf,[1] Jacqueline Mohan,[2] Emily Moran,[1,2] Luke Pangle,[1] Scott Pearson,[1] Carl Salk,[1,2] Zehao Shen,[1] Denis Valle,[1] and Peter Wyckoff[2]

[1]*Nicholas School of the Environment, Duke University, Durham, North Carolina 27708 USA*
[2]*Department of Biology, Duke University, Durham, North Carolina 27708 USA*
[3]*Department of Statistical Science, Duke University, Durham, North Carolina 27708 USA*
[4]*Cary Institute of Ecosystem Studies, Milbrook, New York 12545 USA*

Abstract. High biodiversity of forests is not predicted by traditional models, and evidence for trade-offs those models require is limited. High-dimensional regulation (e.g., *N* factors to regulate *N* species) has long been recognized as a possible alternative explanation, but it has not be been seriously pursued, because only a few limiting resources are evident for trees, and analysis of multiple interactions is challenging. We develop a hierarchical model that allows us to synthesize data from long-term, experimental, data sets with processes that control growth, maturation, fecundity, and survival. We allow for uncertainty at all stages and variation among 26 000 individuals and over time, including 268 000 tree years, for dozens of tree species. We estimate population-level parameters that apply at the species level and the interactions among latent states, i.e., the demographic rates for each individual, every year. The former show that the traditional trade-offs used to explain diversity are not present. Demographic rates overlap among species, and they do not show trends consistent with maintenance of diversity by simple mechanisms (negative correlations and limiting similarity). However, estimates of latent states at the level of individuals and years demonstrate that species partition environmental variation. Correlations between responses to variation in time are high for individuals of the same species, but not for individuals of different species. We demonstrate that these relationships are pervasive, providing strong evidence that high-dimensional regulation is critical for biodiversity regulation.

Key words: Bayesian analysis; biodiversity; coexistence; competition; forest dynamics; hierarchical models.

Introduction

Although many hypotheses to explain biodiversity are debated, none actually predict high diversity, unless supported by continual inoculation of species from somewhere else. Of course, if competition is weak, maintenance of diversity is not hard to explain. But plants do compete intensely, with massive density dependent mortality from seedling to adult (Harper 1977, Harms et al. 2000, Ibáñez et al. 2007). Repeatable patterns in time (Connell and Slatyer 1977, Christensen and Peet 1984, Huston and Smith 1987, Tilman 1988, Pickett 1989, Chapin et al. 1994) and along gradients (Pastor et al. 1984, Tilman 1985, Inouye and Tilman 1988, Papiak and Canham 2006, Silman 2006, Engelbrecht et al. 2007) have focused attention on competition for a small number of resources, such as light, moisture, and several macronutrients (Tilman 1988, Rees et al. 2001, Silvertown 2004). If patterns are observed repeatedly, and only a few limiting factors are pervasive, it is logical to search for a simple explanation. Robust theory has shown that in competition for a small number of resources each species can dominate somewhere on the landscape only if there are precise trade-offs (MacArthur and Levins 1964, Tilman 1982, Kneitel and Chase 2004). Models predict low diversity, because not many species can find a position of dominance along one or a few axes with limited overlap between them (Tilman 1988, 2004, Gravel et al. 2006, Zillio and Condit 2007).

Finding the trade-offs that would be required to provide so many niches in so few dimensions has long been a challenge for community ecology (Hutchinson 1961, Wright 2002). Trade-offs could apply not only to resources, but also to natural enemies (Janzen 1970, Connell 1971, Chase et al. 2002, Wright 2002, Beckage and Clark 2005, Chesson and Kuang 2008, Feeley and Terborgh 2008), life history and demography (Ellner 1987, Tilman 1994, Cadotte et al. 2006), and interactions among them. Simple models provide critical insights on how trade-offs can promote low levels of

Manuscript received 24 August 2009; revised 22 February 2010; accepted 1 March 2010. Corresponding Editor: A. M. Ellison.
[5] E-mail: jimclark@duke.edu

diversity. An explanation for the dozens to hundreds of competitors that can coexist in many forests could build from this important foundation, but requires a different approach. The lack of methods to analyze multiple interactions could be part of the reason why low-dimensional explanations continue to dominate, despite limited evidence for niche differences (Clark et al. 2007*a*, Clark 2009). We consider an alternative, high-dimensional explanation of diversity, one of multiple limitations distributed among individuals in competing populations (Clark et al. 2004, 2007*a*, Marks and Lechowicz 2006). A hierarchical approach is used to synthesize multiple data sets with demographic interactions within and among populations. We demonstrate that distributions of responses among individuals of competing species are as required to promote coexistence. Our results extend beyond speculation that complexity could be important (e.g., Hutchinson 1961) by defining how it would be structured and how it can be estimated.

Hypothesis tests presented here require quantification of interactions at individual and species scales. Coexistence of N competing species requires up to N limiting factors (MacArthur and Levins 1964, Levin 1970, Grover 1994). The "limiting factors" could be defined in many ways, but need not include trade-offs in a few dimensions. Instead of one or a few axes of differentiation partitioned by trade-offs, there could be many axes and interactions between them, obviating the requirement for simple trade-offs. Quantification of so many interactions would be difficult. But, through analysis at both individual and species scales, we can determine whether or not species respond to variation in the unmeasured dimensions in ways that would promote coexistence. Hypotheses we test apply to these two scales.

At the species scale, we test the hypothesis that there are trade-offs in the dimensions traditionally viewed as important (Fig. 1a), but difficult to quantify. The alternative of high-dimensional regulation would show broad overlap when projected on to a few dimensions (Fig. 1c), due to the fact that individuals within populations are regulated by many factors. If variation in Fig. 1c promotes coexistence, responses of individuals of the same species will be more similar than are those of different species (Fig. 1e). A correlation between any two individuals indicates the extent to which they share common responses to environmental fluctuations (insets in Fig. 1e). For example, negative correlations indicate environmental partitioning (Chesson 2000*a*, *b*). However, correlations between species need not be negative to promote diversity, provided that individuals respond to environmental variation more like others of the same species than of different species (Clark 2010). In other words, we require individual-scale data to test for species differences that promote diversity.

At the individual scale we test the hypothesis that there are trade-offs between individuals in terms of effort devoted to growth and fecundity (Fig. 1b). Such patterns could be genetic (Geber 1990, Mangel and Stamps 2001), but need not be (Tatar and Carey 1995, Barker 1998, Primack and Stacy 1998, Silvertown and Dodd 1999, Obeso 2002, Doblhammer and Oeppen 2003, Mair et al. 2003, Dribe 2004, Hurt et al. 2006, Metcalf et al. 2006). In either case, they can result from a trade-off in resource allocation to different activities. One alternative is "winners vs. losers" (Fig. 1d), the possibility that some individuals excel in terms of all demographic rates while others do poorly. A second alternative is that allocation between individuals is also high dimensional and does not show a simple correlation (Fig. 1c).

Information at the individual scale is critical to determine whether or not the structure of variation is consistent with high-dimensional regulation of diversity. Most of the factors affecting physiology, individual health, and population success cannot be directly measured. Belowground dynamics (Huston and DeAngelis 1994, Jobbágy and Jackson 2004), microbially mediated interactions (Bradley et al. 2008, Clark and Hersh 2009), and lagged responses to environmental variation (Oren et al. 1999, Naumburg and Ellsworth 2000) make direct measurement of coexistence mechanisms difficult. Although a given study could not measure all relevant variables, evidence for high-dimensional regulation can still come from analysis of how individuals of different species respond to environmental variation, by revealing the extent to which individuals respond more like (compete more with) others of the same species. Thus, we quantify not only observation errors, but also the variation among individuals and within individuals over time.

The analysis we implement requires two elements: (1) long-term, simultaneous observations of fecundity, growth, and mortality of individual organisms of many species subject to experimentally manipulated resources, and (2) models that coherently admit information from multiple sources at multiple scales, allowing for their relative importance ("weight"), uncertainty, relationships controlling how species respond to resources, and variation among individuals in those responses. Long-term individual level data that include all demographic rates are required (component 1), because high-dimensional controls on diversity would vary within populations, depending on the heterogeneity of conditions that different individuals experience in space and over time. Demographic rates must be inferred simultaneously, because they interact, potentially compensating or amplifying one another. Compensation occurs when some individuals devote more to reproduction, others to growth (Loehle 1987) or when high fecundity subsequently leads to increased density dependent mortality (Yoda et al. 1965, Clark 1992, Weiner et al. 2001). Amplification occurs if healthy individuals grow fast, produce abundant offspring, and suffer high mortality risk, whereas unhealthy individuals do the opposite. With compensation or amplification, population growth rates evaluated from independent estimates of fecundity,

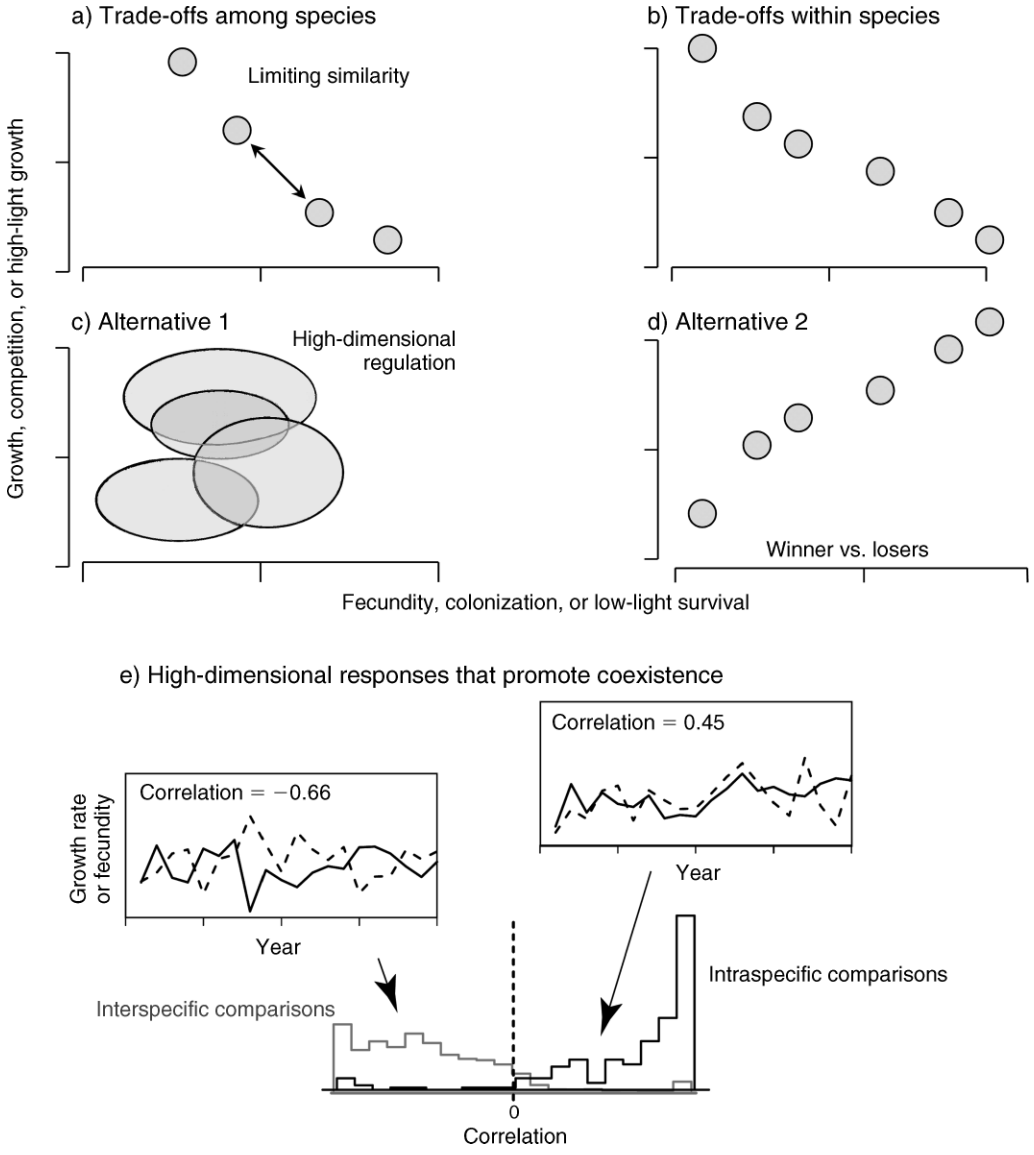

FIG. 1. Hypotheses at two levels for trade-offs involving two traits or demographic rates showing patterns expected from (a) low-dimensional trade-offs among species and (b) within species (among individuals). Alternatives are (c) high-dimensional limitations, which, after accounting for observation error, indicate that limitations are distributed across additional (unobserved) axes, and (d) positive correlations. Alternative 2 is especially relevant within species, where the alternative to trade-offs among individuals can be populations of healthy vs. unhealthy individuals. In panel (e) are example histograms of correlations between individuals in responses that would show partitioning of environmental variation. Correlations between two individuals are shown for the case where correlations are positive and negative. If high-dimensional variation promotes coexistence, then correlations in response should be higher for individuals of the same species than for different species.

growth, and survival are inaccurate. Few long-term data sets include observations of all three demographic schedules from the same individuals, and none that we are aware of analyze their interactions, allowing for uncertainty in the model, variation among individuals and over time, and in error in data.

Experimental manipulation is needed because explanatory variables are often correlated, and observational data rarely provide an adequate range of variation. In our application, tree size and canopy exposure are two correlated explanatory variables that can be separated through manipulation of tree canopies (Dietze and Clark 2008). Although distribution of data (treatments) is a standard consideration for carefully designed experiments, nearly all studies of biodiversity regulation in trees come from purely observational studies, frequently from a single stand, and lacking manipulation, controls, and analysis of covariates.

Models that incorporate multiple sources of information and variation and uncertainty at different scales

(component 2) are critical for synthesis. Where a large number of interactions are important and none overwhelm, there is the possibility of modeling hierarchically, to capture how interactions at one scale, say variation within and among individuals, relate to processes and observations at another, such as among populations and their resources. As described by Berliner (1996, see also Ver Hoef and Frost 2003, Wikle 2003, Clark 2005, Wikle and Berliner 2005, Clark and Gelfand 2006, Royle and Dorazio 2008, Cressie et al. 2009), data at different scales can be coherently assimilated in hierarchical models. Yet there are few ecological examples where multiple sources of information have been successfully exploited for inference on complex interactions. The challenges of building a coherent model, developing efficient algorithms, and evaluation can be daunting. Craigmile et al. (2009) focus on a single large data set, emphasizing the care that is needed at each stage of the analysis. With multiple data sets comes an additional concern, how they contribute simultaneously to inference. Unlike most meta-analyses, which combine information from multiple studies having the same predictors and response variables (Gurevitch and Hedges 1999, Peters and Mengersen 2008), ecologists increasingly wish to combine data sets on different predictors and response variables. Combining data sets requires not only coherency, but also decisions concerning their relative importance or "weight." Despite decades of research involving many approaches, we are unaware of any study that combines these components, in part due to the challenge of formulating a coherent framework for inference. Although the challenges to "computational ecology" are substantial (Pascual 2005), such efforts are critical if there is to be a serious evaluation of the mechanisms that control biodiversity.

Because a large model is critical to evaluation of the biodiversity hypotheses, a second theme of this study concerns how to construct, fit, and evaluate models when data sets and processes are complex. Our approach for synthesis focuses on quantifying factors hypothesized to define low-dimensional niche differences, such as light availability, and the variation that remains after observable factors are included, specifically whether or not that variation is structured among individuals, over time, or both (Clark et al. 2004). We exploit all available evidence to allow for uncertainty at all stages of the model. We apply this approach to unusually extensive long-term experimental data with observations on covariates and demographic responses, including growth, maturation, fecundity, dispersal, and survival. Inference yields not only species-level parameters, but also estimates of demographic rates for 27 000 individuals distributed over 268 000 tree-years (individual observation years) for dozens of species. Results are used to determine the distributions of demographic rates within and between species that critically determine population growth and apply them to the goal of explaining high diversity. We test hypotheses summarized in Fig. 1 for all of the dominant tree species in 11 stands in the southern Appalachians and Piedmont followed for up to 18 years. Because it is not widely appreciated why current models fail to predict diverse assemblages and how the structure of variation analyzed here can provide insight, we first summarize assumptions of current models, in the context of individual success. We follow with a rationale for the specific hypotheses that come from these assumptions and their connections to the modeling approach we adopt.

The relationship between trade-offs and individuals

Trade-offs are needed to promote diversity in low dimensional models, by allowing competitors to share a low-dimensional niche space, partitioning it into different combinations of limitations. A colonization–competition trade-off could allow species to share two dimensions, provided there is a strict trade-off in abilities to colonize and to compete in an environment providing opportunities for both (Fig. 1a), say through new patch formation followed by succession (Hastings 1980, Tilman 1994, Cadotte et al. 2006). A trade-off in low-light survival vs. high-light growth (Denslow 1980, Canham 1988, 1989, Poulson and Platt 1989, Welden et al. 1991, Kobe 1996, Walters and Reich 1996, Dalling and Hubbell 2002, Wright 2002, Baraloto et al. 2005, Valladares and Niinemets 2008) could explain diversity in an environment with variable light.

Where present trade-offs almost certainly contribute to diversity, but empirical support is limited. In the many efforts to quantify trade-offs from field data (Reich et al. 1997, Wright et al. 2004, Gilbert et al. 2006), few suggest the strong negative correlations required by theory (Fig. 1a; but see Tilman 1994 for a clear example). Moreover, simple negative correlation is not sufficient–coexistence further requires that species are too similar to coexist (MacArthur and Levins 1967, Abrams 1988), although it may be difficult to define the limit to similarity (Meszéna et al. 2006). Evidence for such differences would look like Fig. 1a, a pattern that is rarely observed in data (Clark et al. 2007a, Clark 2009).

Including stochastic terms can increase diversity in some types of models (Chesson 2000*a*, *b*, Volkov et al. 2003, Lichstein et al. 2007), but typically not by much. Despite slowing exclusion in some cases, stochastic simulations still predict modest levels of diversity (Tilman 1988, 2004, Pacala and Tilman 1994, Gravel et al. 2006), unless explicit competitive advantages are provided for each species somewhere on the landscape (e.g., Hurtt and Pacala 1995). Effects of stochasticity can be weak or even negative, depending on how it is implemented, and high diversity requires a continual inoculation of species (Shugart 1984, Hubbell 2001). The stochasticity in such models is the surrogate for unspecified niche differences, providing each competitor with times and locations where it does well and others do poorly. The implicit niche differences prolong competitive exclusion, effectively allowing for negative correla-

TABLE 1. Calculations from latent states diameter growth rate, fecundity potential, and mortality risk.

Demographic rate	Species mean	Individual mean (over years)	Variance among individuals	Annual mean (over individuals)	Annual variance
Diameter growth rate	$\overline{d} = \dfrac{\sum_{ij,t} d_{ij,t} z_{ij,t}}{\sum_{ij,t} z_{ij,t}}$	$\overline{d_{ij}} = \dfrac{\sum_{t} d_{ij,t} z_{ij,t}}{\sum_{t} z_{ij,t}}$	$\dfrac{\sum_{ij} (\overline{d_{ij}} - \overline{d})^2}{n-1}$	$\overline{d_t} = \dfrac{\sum_{i,j} d_{ij,t} z_{ij,t}}{\sum_{i,j} z_{ij,t}}$	$\dfrac{\sum_{i,j} d_{ij,t}^2 z_{ij,t}}{\sum_{i,j} z_{ij,t}} - \overline{d}^2$
Fecundity potential	$\overline{f} = \dfrac{\sum_{ij,t} f_{ij,t} Q_{ij,t} z_{ij,t}}{\sum_{ij,t} Q_{ij,t} z_{ij,t}}$	$\overline{f_{ij}} = \dfrac{\sum_{t} f_{ij,t} Q_{ij,t} z_{ij,t}}{\sum_{t} Q_{ij,t} z_{ij,t}}$	$\dfrac{\sum_{ij} (\overline{f_{ij}} - \overline{f})^2}{n-1}$	$\overline{f_t} = \dfrac{\sum_{i,j} f_{ij,t} Q_{ij,t} z_{ij,t}}{\sum_{i,j} Q_{ij,t} z_{ij,t}}$	$\dfrac{\sum_{i,j} f_{ij,t}^2 Q_{ij,t} z_{ij,t}}{\sum_{i,j} Q_{ij,t} z_{ij,t}} - \overline{f}^2$
Mortality risk	$\overline{\zeta} = \dfrac{\sum_{ij,t} \zeta_{ij,t} z_{ij,t}}{\sum_{ij,t} z_{ij,t}}$	$\overline{\zeta_{ij}} = \dfrac{\sum_{t} \zeta_{ij,t} z_{ij,t}}{\sum_{t} z_{ij,t}}$	$\dfrac{\sum_{ij} (\overline{\zeta_{ij}} - \overline{\zeta})^2}{n-1}$	$\overline{\zeta_t} = \dfrac{\sum_{i,j} \zeta_{ij,t} z_{ij,t}}{\sum_{i,j} z_{ij,t}}$	$\dfrac{\sum_{i,j} \zeta_{ij,t}^2 z_{ij,t}}{\sum_{i,j} z_{ij,t}} - \overline{\zeta}^2$

Notes: Variables for individual i in stand j in year t are fecundity ($f_{ij,t}$), diameter increment ($d_{ij,t}$), maturation status ($Q_{ij,t}$), mortality risk ($\zeta_{ij,t}$), and live status ($z_{ij,t}$). Means are indicated with overbars.

tions in recruitment success (Clark et al. 2007*a*, Clark 2009). Although negative correlations between species in their responses to variation would tend to promote diversity (Chesson 2000*a*, Clark et al. 2007*a*), many species do not show negative correlation, as expected if they are, on average, limited by similar factors (Clark 2010). For example, many species benefit from canopy gaps and from increased moisture availability in wet years. Simple random noise in models does not provide an answer to high diversity in nature, because nature does not provide the low-dimensional niche differences supplied by stochastic terms in such models. Missing processes must be taken up by stochastic terms, but how stochasticity enters models can determine whether or not it might stand in for actual species differences. Thus, variation needs to be quantified at several levels.

High-dimensional limitation will be expressed, in part, through individual differences and over time (Clark et al. 2004, 2007*a*). Let $c_d(i, i')$ be the correlation in growth rate d between individuals i and i', calculated as in Tables 1 and 2. Two such comparisons are illustrated in Fig. 1e. If individuals are limited by the same factors, variation in these factors would produce positively correlated responses in d: the two individuals tend to grow well under the same conditions, and vice versa. If individuals are limited by different factors, then correlations will tend to be low, possibly even negative, as fluctuations in those factors cause different responses in the two individuals. However, to promote diversity high-dimensional regulation does not require negative correlation between species abundances, only that correlations among individuals of the same species exceed those for individuals of different species (Fig. 1e). This would be evidence that species partition the environment. Evaluation requires simultaneous inference on demographic rates at the level of individuals and years, using models that contain more complexity than is typical in ecology. In the next section, we address how and why a large model can guide understanding of high-dimensional interactions.

The scale of inference and implications for understanding coexistence

Large models require justification. They can be intractable and difficult to parameterize, to evaluate, and to understand. Motivation comes from failure of

TABLE 2. Correlations between demographic rates.

Correlation between individuals, diameter growth	$c_d(i,i') = \sum_t (d_{ij,t} - \overline{d_{ij}})(d_{i'j,t} - \overline{d_{i'j}}) z_{ij,t} z_{i'j,t} \Big/ \left(s_d(i) s_d(i') \sum_t z_{ij,t} z_{i'j,t} - 1 \right)$
Correlation between rates, individual ij	$c_{ij}(d,f) = \sum_t (d_{ij,t} - \overline{d_{ij}})(f_{ij,t} - \overline{f_{ij}}) z_{ij,t} Q_{ij,t} \Big/ \left(s_d(i) s_f(i) \sum_t Q_{ij,t} z_{ij,t} - 1 \right)$
Correlation within individual, lag l	$c_l(d,f) = \sum_t (d_{ij,t-1} - \overline{d_{ij}})(f_{ij,t-l} - \overline{f_{ij}}) z_{ij,t} Q_{ij,t} \Big/ \left(s_d(i) s_f(i) \sum_t Q_{ij,t} z_{ij,t} - 1 \right) >$

Note: The standard deviation for variable v for individual i is $s_v(i)$, the correlation between individual i and i' is $c_v(i, i')$ (Figs. 22 and 23); the correlation between variables v and v' for individual ij is $c_{ij}(v, v')$ (Figs. 19 and 20).

simple models because they leave out too many important relationships. Despite the widely recognized limitations of large models, they have become standard tools where many processes contribute and none overwhelm: weather prediction, climate dynamics, gene interactions, biochemical networks, and granular flows are examples (O'Hagan and West 2010). Ecologists have argued for more sophisticated treatment of complexity (Levin 1998, Clark 2005, Pascual 2005), including biodiversity (Dunne et al. 2002, Clark et al. 2007*a*, Clark 2009). However, we are unaware of simultaneous inference at multiple levels, including individual-level, long-term, and multi-cohort data. An inferential effort as extensive as ours is novel, so we summarize the rationale, emphasizing the scale of inference adopted here as motivation for the modeling approach that follows.

A principle motivation for this effort is the limited progress that has come from simple analyses. If the weak trait correlations observed from empirical study are not consistent with predictions from simple models, then how can a larger model help? First, is the need to separate variation associated with processes versus observation (Berliner 1996, Clark 2005, Ogle 2009). If large variation in Fig. 1c results from observation error, then it cannot contribute to coexistence.

At the process level, trade-offs might exist (1) among species having different resource requirements and life history constraints and (2) among individuals within a population subject to different limitations and possessing different genotypes. Variation at these levels has different implications. Where species abundances are treated as observations, correlations between species can suggest trade-offs where they do not exist, and vice versa. Species most abundant on the best sites can have high mortality rates simply because stand-level mortality compensates for rapid growth (Assmann 1970, Clark 1992, Silvertown et al. 1993). Then comparisons between species show positive growth–mortality correlation not due to a trade-off, but rather due to other factors that control where they occur. Species comparisons can show differences on average (i.e., means are "significantly different"), despite the fact that individuals of those species collectively overlap (Fig. 1c). Species averages may not differ (e.g., Condit et al. 2006), despite the fact that the individuals of different species are responding to the environment in different ways (Fig. 1e). This occurs when individuals within a species are responding to unobserved variables, which can be inferred only if there are individual-level data (Clark et al. 2003, 2004).

Inference on high-dimensional regulation requires individual-year ("tree-year") observations. In the aforementioned example of compensation (typical in thinning stands), a negative correlation between growth rate and survival at the species level (thinning is rapid on the best sites) belies the underlying positive relationship at the individual level: healthy individuals grow rapidly and suffer low mortality risk (Kobe 1996, Wyckoff and Clark 2000). The so-called "ecological fallacy" (Kramer 1983, Ibáñez et al. 2006, Clark 2007) comes from a mismatch between scales of data and inference. Proper inference requires analysis of the distribution of individual health across each population. Replicated observations at the individual level (Hurt et al. 2006, Ricklefs and Cadena 2007) can show if variation results from species responding to variation in different ways. It can thus be valuable to include covariates directly into the analysis (e.g., Russo et al. 2008). Here we do so at the level of demographic rates for individuals and species to determine the basis for species differences.

Hierarchical modeling provides a means for inference at different scales (Wikle 2003, Clark 2005, Latimer et al. 2006, Cressie et al. 2009, Ogle 2009). To address these complications we model simultaneously the demographic schedules within and between individuals for all species. We obtain a coherent assimilation of multiple data types, and quantify underlying connections between demographic rates both within and among individuals over time (Table 1).

Study Sites and Design

The stands analyzed in this study span moisture and elevation gradients in the southern Appalachians (Coweeta Hydrologic Lab, Macon County), the Piedmont (Blackwood Division, Chapel Hill), and the transition between them (Mars Hill, Madison County), of North Carolina (Fig. 2; Table 3). The three regions were selected to include a range of climates (including elevation), parent material, and soil moisture. Piedmont plots (DB, DH) occupy mixed hardwood and pine stands on soils characterized by low organic matter, with a range of water-holding capacities, and low to high shrink-swell clays. Southern Appalachian plots (C1, C2, C3, C4, C5, CL, CU) occupy elevations from 780 to 1410 m in the Blue Ridge Belt of southwestern North Carolina, spanning low-elevation mixed oak (700 m) to high-elevation (>1400 m) northern hardwood and moist cove forest to xeric ridge tops. Soils differ in cation exchange, pH, and drainage. Mars Hill plots (MP, MF) are transitional, being lower in elevation than Southern Appalachian sites and comparable in climate. Some species occur in only a portion of the study region (acronyms in Table 4), others occur at all sites (Table 5). Plots were first established between 1992 and 2004.

Data come from an intervention design for canopy gap manipulation that allows for pre-treatment/post-treatment comparisons, provides a range of variation in light availability needed to parameterize its effects, and creates conditions required for recruitment of gap specialists (Canham 1988, 1989, Cole and Lorimer 2005). Of the 11 study plots, three were designated for experimental canopy manipulation (CL, CU, DB), made sufficiently large to allow for experimental canopy gaps with intervening continuous forest. Design and implementation of gaps is detailed in Dietze and Clark (2008). The intervention design provides pretreatment data for trees,

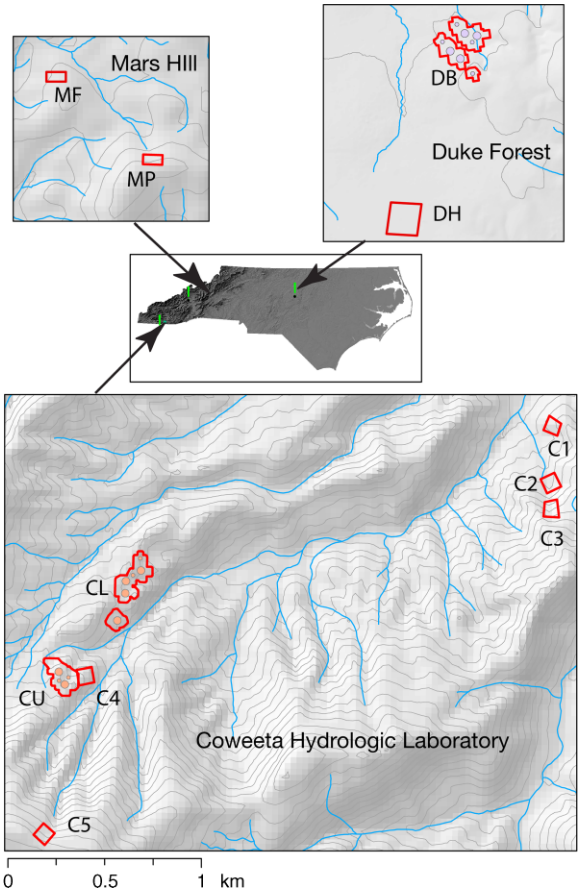

FIG. 2. Three study regions in Blue Ridge (Coweeta), Transition (Mars Hill), and Piedmont (Duke Forest), showing plots outlined in red and experimental canopy gaps (circles; Table 2). Contours are 20 m. Inset maps have a common vertical and horizontal scale.

TABLE 4. Species codes used in other tables and figures.

Code	Species
acru	*Acer rubrum*
acsa	*Acer saccharum*
acpe	*Acer pensylvanicum*
acba	*Acer barbatum*
beal	*Betula alleghaniensis*
bele	*Betula lenta*
caca	*Carpinus caroliniana*
cagl	*Carya glabra*
caov	*Carya ovata*
cato	*Carya tomentosa*
ceca	*Cercis canadensis*
cofl	*Cornus florida*
fagr	*Fagus grandifolia*
fram	*Fraxinus americana*
list	*Liquidambar styraciflua*
litu	*Liriodendron tulipifera*
nysy	*Nyssa sylvatica*
oxar	*Oxydendron arboreum*
piri	*Pinus rigida*
pist	*Pinus strobus*
pita	*Pinus taeda*
piec	*Pinus echinata*
pivi	*Pinus virginiana*
qual	*Quercus alba*
quco	*Quercus coccinea*
qufa	*Quercus falcata*
quma	*Quercus marilandica*
quph	*Quercus phellos*
qupr	*Quercus montana*
quru	*Quercus rubra*
qust	*Quercus stellata*
quve	*Quercus velutina*
rops	*Robinia pseudoacacia*
tiam	*Tilia americana*
tsca	*Tsuga canadensis*
ulal	*Ulmus alata*
ulam	*Ulmus americana*
ulru	*Ulmus rubra*

seed collections, and environmental data and continued after gaps were created in 2001. We therefore have trees that have continuously grown at all sites without intervention, many exposed to the intervention (left standing in and at the edges of gaps), and others that experienced changes in canopy characteristics without intervention, due to continuing stem mortality.

METHODS

Our goal is to quantify interactions between demographic rates, within individuals, between individuals, and between species, as they respond to environmental

TABLE 3. Study sites, including location, parent material, soils, and treatments by plot.

	Blue Ridge plots (Coweeta Hydrologic Lab)†							Transition plots (Mars Hill)‡		Piedmont plots (Duke Forest)§	
Parameter	C1	C2	C3	C4	C5	CL	CU	MP	MF	DB	DH
Elevation (m)	780	820	870	1110	1410	1030	1140	710	770	155	170
Area (ha)	0.64	0.64	0.64	0.64	0.64	2.75	1.45	0.5	0.5	4.11	2.40
First year	1992	1992	1992	1992	1992	2000	2000	2004	2004	2000	1999
Gap treatment	C	C	C	C	C	C, 4L, 2S	C, 4L, 2S	C	C	C, 4L, 2S	C, 4L, 2S

Note: Gap treatments are: C, control only; L, large (40 m diameter); S, small (20 m diameter).

† Mean annual temperature is 12.7°C; mean annual precipitation is 1780–2500 mm (ranging from low elevation to high); location is 35°03′ N, 83°27′ W; Blue Ridge Belt lithotectonic region.

‡ Mean annual temperature is 11.6°C; mean annual precipitation is 1020 mm; location is 35°49′ N, 82°32′ W; Blue Ridge Belt lithotectonic region.

§ Mean annual temperature is 14.6°C; mean annual precipitation is 1210 mm; location is 35°58′ N, 79°05′ W; Triassic Basin lithotectonic region.

TABLE 5. Basal area (m2/ha) of species included in this analysis, ranked by weighted average against plot elevation.

	Piedmont plots		Transition plots		Blue Ridge plots						
Species	DH, 165 m	DB, 170 m	MF, 720 m	MP, 730 m	C1, 780 m	C2, 820 m	C3, 870 m	CL, 1030 m	C4, 1110 m	CU, 1140 m	C5, 1410 m
ulru	0.31	0	0	0	0	0	0	0	0	0	0
quph	3.8	0.36	0	0	0	0	0	0	0	0	0
qust	2.74	0.5	0	0	0	0	0	0	0	0	0
acba	0.14	0.04	0	0	0	0	0	0	0	0	0
ulam	0.28	0.09	0	0	0	0	0	0	0	0	0
ulal	1.17	0.72	0	0	0	0	0	0	0	0	0
pita	12.84	14.34	0	0	0	0	0	0	0	0	0
qufa	0.58	0.7	0	0	0	0	0	0	0	0	0
list	4.26	5.29	0	0	0	0	0	0	0	0	0
pivi	0.03	0.21	0	0	0	0	0	0	0	0	0
ceca	0.02	0.18	0	0	0	0	0	0	0	0	0
piec	0.03	1.38	0	0	0	0	0	0	0	0	0
caca	0.27	0.07	0.01	0.02	0	0	0	0	0	0	0
cato	0.18	1.53	0	0	0	0	0	0.33	0	0.03	0
caov	0.64	0	0	0	0	0	0.31	0	0	0	0
qual	2.57	4.89	11.64	1.69	0.61	0	0	0	0	0	0.23
cofl	0.31	0.79	0.11	0.67	0.32	0.92	0.39	0.27	0.14	0.06	0.01
pist	0	0	2.37	0.83	0.03	0.03	0	0	0	0	0
fagr	0	0.01	5.77	1.14	0.07	0.01	0	0	0	0	0.41
piri	0	0	0	0	5.33	0	0	0	0	0	0
fram	1.9	0.8	0.02	1.41	0	0	0.07	0.04	0.76	0	2.36
quve	0	0.56	1.69	1.08	1.7	1.8	1.7	0.1	0.25	0.63	0
litu	1.15	3.75	3.05	1.75	0.13	7.83	1.08	13.12	0.05	0.05	0
cagl	0.66	0.72	0.13	0.7	1.59	3.83	3.87	0.74	1.43	0.11	0.13
acru	2.71	3.36	3.86	2.24	4.48	6.14	6.11	9.42	8.44	11.19	0.26
nysy	0.82	0.37	0.66	1.14	1.03	0.85	4.35	1.58	3.22	2.96	0
quco	0	0	4.23	0.34	2.77	2.87	0.14	2.38	1.82	3.57	0
quma	0	0	1.11	20.17	5.8	4.6	14.77	6.68	11.69	11.06	0
rops	0	0.06	0	0	1.13	1.31	0.43	0.97	0.57	0.72	0
oxar	0	0.37	1.34	1.69	2.53	1.06	4.21	1.07	4.38	4.27	0
tsca	0	0	0	0	0.04	0.77	0.11	1.56	0.97	0.28	0.21
quru	0	0.68	0.39	1.98	2.88	1.3	3.98	6.42	6.21	2.7	7.31
bele	0	0	0	0	0.06	2.56	0.43	0.16	0.13	0.01	7.03
acpe	0	0	0	0	0.02	0.38	0.15	0.19	0.37	0.05	1.7
acsa	0	0	0	0.02	0	0.33	0	0.11	0	0	1.74
tiam	0	0	0	0	0	0.37	0	0	0	0	6.8
beal	0	0	0	0	0	0.05	0.08	0	0	0	9.89
Total	37.43	41.77	36.39	36.86	30.51	37	42.19	45.14	40.45	37.7	38.08

Note: For key to species abbreciations, see Table 4.

covariates, here including tree size and light availability. In addition to equations and parameters, the model contains state variables and observations. State variables are diameter D, diameter growth d, maturation probability θ, maturation status Q, fecundity f, mortality risk ζ, and exposed canopy area (ECA) λ and are shown in Fig. 3. In principle, some state variables might be directly observed and thus are "known," others will be partially observed, observed with error, or unobserved, in which case they must be estimated along with parameters. These estimated state variables are *latent states*. In the current application, state variables must be estimated, with information coming from observations (Fig. 3), prior knowledge of observation errors, and the full process model. Data sets include diameter censuses $D^{(o)}$, increment cores $d^{(o)}$, seed traps s, remote sensing and canopy status observations (summarized as $C^{(o)}$ in Fig. 3), maturation q_t and (for dioecious species) gender h_t status observations, and survival status z_t. The observations are obtained in the context of canopy intervention experiments (Dietze and Clark 2008), summarized in this analysis by their effects on light availability, the ECA λ.

Data on tree growth (Clark et al. 2007*b*), survival (Wyckoff and Clark 2002, Metcalf et al. 2009), canopy exposure to light (Wyckoff and Clark 2005), and maturation and fecundity (Clark et al. 2004) were collected from each of the 11 plots for a period of 5 to 17 years (Tables 6 and 7), including pretreatment for gap experiments (Dietze and Clark 2008, Ibáñez et al. 2009). Observations come from $i = 1, \ldots, n_j$ trees on plots $j = 1, \ldots, J$ plots, where $J = 11$ (Table 3). Each tree has a unique history of observations. An individual is first observed in year t_{ij}, either the year when a sample plot was established or when the tree first became large enough to be included in the census (2 m in height). The last year it is observed is T_{ij}, which is 2008 or the year of death or censoring (trees pulled down for the canopy experiment).

Tree measurements are similar to those available from large tree plots in the tropics, with some additional

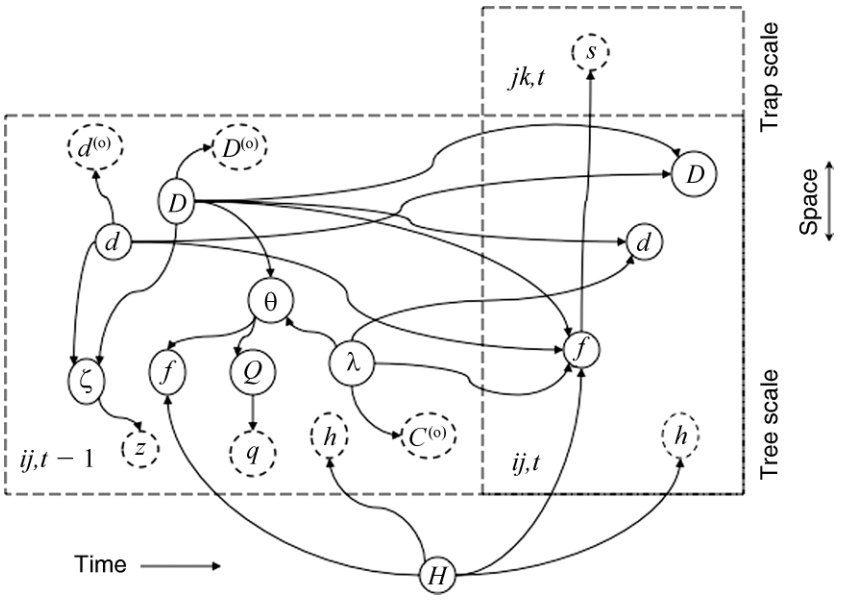

FIG. 3. A simplified directed acyclic graph of interactions and data for tree i in forest stand j in year t. Latent states include diameter D, diameter growth increment d, maturation probability θ, maturation status Q, fecundity f, gender H, mortality risk ζ, and light availability λ. Data include growth increment data $d^{(o)}$, diameter measurements $D^{(o)}$, survival observations z, maturation observations q, gender observations h, and canopy observations $C^{(o)}$. Boxes in dashed outline indicate state variables for tree i in stand j in year $t-1$ (ij, $t-1$: all state variables shown), in year t (ij, t: a subset of variables shown), and in seed trap k in stand j in year t (jk, t). Seed trap data s are at the 1-m scale, rather than tree scale.

categories. All trees greater than 2 m in height are identified to species and locations mapped (x, y, z). Individual measurements obtained at the time of censuses include diameter, canopy status, reproductive status (which includes maturation and gender status), and survival (Fig. 3). Trees are remeasured at 2–4 year intervals. Mortality and ingrowth (i.e., the addition of new individuals 2 m in height) are recorded at each census. Increment cores are extracted and annual growth rates (ring widths) measured from a sample of species and size classes at regular intervals to provide an estimate of annual growth increment. For purposes of evaluating results, we measured ring widths not only for the study period and sample plots, but also for the full growth histories of trees within and outside sample plots. These were used when we predict growth against age, although age is not used to fit the model.

There are seed traps $k = 1, \ldots, K_j$ distributed throughout each stand j, but with additional traps concentrated near canopy gaps in treatment plots (Fig. 4), which provide spatiotemporal seed counts. Data collection methods for trees and seeds are detailed in Clark et al. (1998, 2004) and for diameter growth and mortality in Wyckoff and Clark (2000, 2005) and Clark et al. (2007*b*).

Maturation status is given by the indicator $Q_{ij,t} = 0$ (immature) or 1 (mature) and gender by the indicator $H_{ij} = 0$ (male) or 1 (female). Observations of reproductive status are $q_{ij,t}$ for maturation and $h_{ij,t}$ for gender (Table 8). Observation categories for individual i on plot j in year t, or ($q_{ij,t}$, $h_{ij,t}$) are "uncertain," "not reproductive" (whole crown visible, no reproduction observed), "flowering" (for dioecious species, gender unknown), "seeds/fruit" (mature and female), "male" (flowers sometimes identified as male), and "female." To maximize detection, reproductive status is recorded during the flowering season, the fruiting season, or both, depending on species, because visibility is restricted (Clark et al. 2004). Dioecious species (*Acer rubrum*, *A. pennsylvanicum*, *Fraxinus americana*, *Nyssa sylvatica*) include individuals lacking female function. All mature individuals of monoecious species have both male and female function. The relationship between observations, and maturation and gender status are given in Table 8.

To allow for an extended pretreatment period canopy gaps were created two years after data collection began (Table 3), by pulling all dominant and codominant trees within the designated gap areas of 20 m and 40 m diameters with a skidder (Dietze and Clark 2008). There were a total of 10 large and 8 small gaps. At all sites, control treatments included all areas not influenced by gaps.

Model rationale

We rely on model-based inference at the level of individual trees, represented by estimates of latent states, each responding to a different set of local and regional conditions and including year-to-year variation. The population response emerges as a collection of individual responses, summarized by fitted parameters, with detail coming from estimates of latent states (Clark and LaDeau 2006). An individual tree is characterized by

TABLE 6. Tree-scale data, shown as dashed circles in Fig. 3.

			Increment cores					Reproductive status					Canopy status			
Species	Trees	DCens	IncCr	IncYr	Died	InGro	GapTm	RepUn	RepNo	Rep	RF	RM	Can1	Can2	Can3	CanRe
acru	6600	43 828	347	5080	824	1507	865	14 304	1605	892	632	545	7796	1060	377	142
acsa	143	1124	14	334	12	53	5	357	10	9	0	0	101	11	4	48
acpe	821	6190	27	536	107	423	50	2473	16	21	23	8	599	54	23	78
acba	131	616	2	30	5	69	6	198	30	2	0	0	264	9	1	0
beal	160	1589	34	586	35	21	0	482	33	63	0	0	50	33	16	72
bele	163	1422	37	766	24	39	16	540	8	85	0	0	32	63	19	28
caca	590	2526	2	32	30	393	34	551	40	37	9	0	973	67	8	0
cagl	416	3518	108	1850	48	32	32	1140	103	110	0	0	370	116	64	676
caov	68	370	5	90	6	24	0	155	5	19	2	0	116	22	6	0
cato	493	3470	75	996	48	52	73	1074	218	107	0	0	676	119	51	1584
ceca	321	2058	12	178	64	34	35	581	13	133	0	0	595	34	8	0
cofl	2342	13 168	45	840	716	414	283	4619	51	243	1	0	3492	215	23	8
fagr	263	1281	20	296	12	43	7	156	0	1	0	0	251	27	5	82
fram	1607	8083	41	700	213	725	129	2244	28	9	49	0	2497	168	53	40
list	2169	11 957	119	1426	217	877	252	3115	1675	315	0	0	2596	483	159	0
litu	1243	7948	156	2054	190	269	187	2843	424	367	0	0	1011	290	256	2
nysy	1841	12 854	60	1092	213	447	164	5074	71	3	25	0	2366	235	87	32
piri	36	432	18	344	4	0	0	73	0	31	0	0	2	3	23	58
pist	136	516	12	96	17	22	0	14	0	3	0	0	110	5	2	0
pita	566	3354	117	1484	113	130	68	842	47	722	0	0	53	335	253	0
piec	77	469	19	242	32	2	12	131	3	93	0	0	1	46	29	0
pivi	26	146	5	54	13	1	0	53	0	25	0	0	1	9	5	0
qual	346	2202	138	1694	62	30	38	676	5	104	10	0	133	205	119	6
quco	140	1057	27	570	23	13	18	478	3	43	0	0	8	20	47	30
qufa	26	164	12	128	5	4	4	46	0	8	0	0	4	13	10	0
quph	91	482	11	120	10	34	0	183	0	24	4	0	23	53	37	0
qupr	731	6130	130	1766	112	53	81	2747	10	44	0	0	124	151	211	22
quru	406	3134	113	1592	80	35	54	1337	11	105	0	0	141	81	97	18
qust	83	490	14	150	8	27	7	140	1	11	0	0	30	62	26	0
quve	123	882	33	624	36	17	8	323	0	31	0	0	50	30	23	34
rops	155	1062	18	472	39	49	10	576	2	3	0	0	55	20	19	12
tiam	93	790	16	350	29	33	0	318	0	0	0	0	39	8	12	48
tsca	378	3420	35	734	10	54	55	1381	114	17	0	0	333	32	16	0
ulal	1275	7196	42	636	66	487	78	1801	543	92	0	0	2108	131	23	0
ulam	216	1022	3	50	8	147	1	170	65	8	0	0	348	37	0	0
ulru	64	426	0	0	4	6	0	213	7	7	0	0	163	15	4	0
Total	24 339	155 376	1867	27 992	3435	6566	2572	51 408	5141	3787	757	559	27 511	4262	2116	3020

Note: Abbreviations are: Trees, number of trees observed; DCens, number of diameter measurements taken; IncCr, number of increment cores; IncYr, number of increments measured; Died, number of trees that died during the study interval; InGro, number of trees that entered the study, first reaching a height of 2 m during the study interval, 1992–2009; GapTm, number of trees benefiting from increased light with creation of experimental canopy gaps; RepUn, number of observations where an individual was designated as unknown reproductive status; RepNo, number of observations where an individual was designated as not reproductive; Rep, number of observations where an individual was designated as reproductive; RF, number of observations where an individual was designated as female (dioecious species); RM, number of observations where an individual was designated as male (dioecious species); Can1, number of trees designated as suppressed canopy stature; Can2, number of trees designated as intermediate canopy stature; Can3, number of trees designated as codominant canopy stature; CanRe, number of trees for which there are remote-sensing estimates of exposed canopy area (includes only individuals that could be confidently identified on the ground). See Table 4 for key to species abbreviations.

continuous (diameter, diameter increment, crown area, fecundity, mortality risk) and discrete (live/dead, immature/mature, and, for dioecious species, male/female) latent states, each of which is partially known. There is thus a multivariate vector of states for individual i on plot j in each year t, $\mathbf{S}_{ij,t} = [d, D, \lambda, \theta, Q, H, f, \zeta, z]_{ij,t}$ including, respectively, diameter growth increment (mm), diameter (cm), exposed canopy area (m^2), maturation risk (probability), maturation status (0, 1), gender (0 male, 1 female), fecundity (number of seeds), mortality risk (probability), and survival (0, 1). The states are modeled together, collectively responding to the individual's environment, which changes from year to year (Fig. 3). Thus we have thousands of nonlinear, multivariate state–space models, one for each tree, characterized by both shared and individual responses to their local environment and fluctuations. To limit complexity, the directed graph for the model shown in Fig. 3 includes only the demographic rates that are represented as state variables in the model and observations; it does not include parameters.

Although more complex than is typically used for inference, the model actually contains a minimal number of relationships. Parameter-level hypothesis testing is obviated by the fact that the model only contains interactions already known to be important. For example, it is known that plant vigor responds to light, that demographic rates interact, and that models can

TABLE 7. Seed trap data for each plot, shown in Fig. 4.

Species	C1 (340)	C2 (340)	C3 (340)	C4 (340)	C5 (340)	CL (633)	CU (385)	BW (1016)	HW (378)	MF (175)	MP (180)	Total (4467)
Acer	3552	5392	5481	8611	4379	8019	6805	15 935	3241	327	72	219.8
Betula	1219	25 713	12 080	2636	329 179	2210	4065	1	0	0	2	2920.9
Carpinus	0	0	0	0	0	0	0	199	878	1	0	3.1
Carya	48	95	309	29	13	44	5	110	140	2	7	4.4
Cercis	0	0	0	0	0	0	0	223	3	26	3	0.6
Cornus	155	48	4	4	3	4	17	252	94	2	8	2.5
Fagus	0	1	0	0	0	0	0	0	0	179	5	0.3
Fraxinus	0	9	0	3	763	1	2	3183	907	1	6	13.9
Liquidambar styraciflua	0	0	2	0	0	3	4	14 620	3639	0	0	45.0
Liriodendron tulipifera	228	15 539	2814	696	58	9418	69	27 291	2295	372	1220	233.4
Nyssa	538	63	2277	1565	2	131	52	27	88	0	37	22.6
Oxydendron	5097	200	1648	3740	1	1005	6977	525	2	201	39	87.8
Pinus	322	11	13	1	3	32	0	9980	3075	288	87	38.1
Quercus	522	244	574	1671	1796	273	253	1782	2475	224	126	51.1
Robinia	11	1	4	5	0	35	23	15	1	0	0	0.2
Tilia	2	808	3	2	832	0	0	0	2	0	0	11.7
Tsuga	14	18	16	105	8	958	81	0	0	0	0	3.6
Ulmus	0	0	5	1	0	0	0	3705	6915	0	0	27.7

Notes: Numbers in parentheses in column headings are trap years. Values in cells for plots are the numbers of seeds recovered from seed traps. Values in cells for Total are the mean numbers of seeds·m^{-2}·yr^{-1}.

capture only a small part of the variance in data. Complexity comes from the fact that we combine them, and we allow for uncertainty in their relationships to one another. We fully exploit prior information, combining theory (e.g., allometric relationships) and previous observations. We use weak priors where data should dominate.

The structure summarized in Fig. 3 differs from other analyses that involve more than one type of data or demographic rate, in that the graph is "fully connected": responses are also predictors. This comes from the fact that latent states have uncertainty, and estimates for all components respond to information coming from all data sources and all parts of the model. If state variables are taken to be fixed, we effectively "break" the graph at each of the nodes in Fig. 3, and each part of the graph is fitted and behaves independently. This approach can provide valuable insights, but we chose here to treat demographic rates synthetically based on all information.

It is important not only to include what is known in advance, but also to identify how priors and data sets contribute to the fit. Large models are difficult to analyze. Extensive analyses with each of the main components of this model preceded the synthetic analysis here, including diameter growth (Clark et al. 2007*b*, Metcalf et al. 2009*a*), survival (Clark et al. 2007*b*, Metcalf et al. 2009*b*, Vieilledent et al. 2009), and

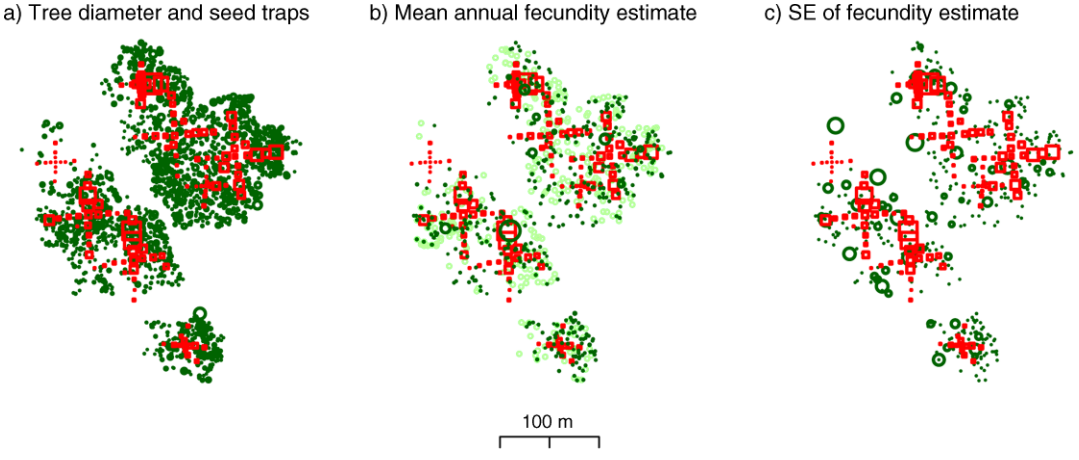

FIG. 4. Example of the mapped plot DB used for demographic inference. (a) Stems of the genus *Acer* (green circles scaled to tree diameter) and seed traps (red boxes scaled to average annual seed collection). (b) Tree symbols scaled to the mean fecundity estimate averaged over years, $\ln[f_{ij,t}] = 9.7$. Light green symbols are trees estimated to have remained immature with probability $>$ 0.5. (c) Tree symbols scaled to average standard error for the annual fecundity estimates (3.7).

TABLE 8. Indicators and probabilities of maturity and gender conditional on observations.

Observation	Maturity indicator $q_{ij,t}$	Maturity probability $\Pr(Q_{ijt} = 1 \mid q_{ij,t})$†	Gender indicator $h_{ij,t}$	Gender probability $\Pr(H_{ij} = 1 \mid h_{ij,t})$†,‡
No observation		$\theta_{ij,t}$		ϕ
Uncertain	0	$\frac{(1-v)\theta_{ij,t}}{1-v\theta_{ij,t}}$	0	ϕ
Not mature	−1	0	0	ϕ
Flowering	1	1	0	ϕ
Seeds/fruits	1	1	1	1
Male or female flowers	1	1	0 or 1	0 or 1

Note: Q is maturation status, H is gender status, q and h are canopy maturation and gender status observations, respectively, at time t for i trees on j plots.

† The probabilities are shown for the special case that there is a single observation per individual. In fact, there are multiple status observations, the modeling of which is discussed in *Methods*. Symbols are: θ, the probability of being in the mature state; v, the probability of detecting mature status; ϕ, the female fraction of the population.

‡ Gender status is assumed static (H has subscript ij), whereas there are multiple observations of status for each individual (h has subscript ij,t).

fecundity (Clark et al. 2004, LaDeau and Clark 2006). For evaluation, we discuss why standard information criteria are not helpful and emphasize instead direct comparisons of priors and posterior distributions, sensitivity analysis, and simulation. We place emphasis on predictive distributions, i.e., simulation models that take posterior distributions as inputs and predictions of latent variables or observations as output. Here we describe data submodels, the full synthetic model, followed by computation, and diagnostics.

Data models

Data for covariates.—Covariates in the model include tree diameter, annual diameter growth increment, and light availability (exposed canopy area or ECA; Wyckoff and Clark 2005), all of which contain observation error. Because of the large number of data types involved (diameter measurements, tree-ring measurements, canopy status observations, remote sensing, and solar geometry model output), we integrate data as a two-step process. First, we inferred tree diameter and canopy exposure in the form of posterior distributions. These posterior distributions are then treated as prior distributions for the full analysis discussed here. The uncertainty in prior distributions thus incorporates the posterior precision from step one (Fig. 5). Here we briefly summarize the first steps, which are detailed in other publications.

Diameter measurements $D^{(o)}_{ij,t}$ and tree-ring data $d^{(o)}_{ij,t}$ (Fig. 3) were combined to obtain posterior distributions of diameter and diameter growth rate for every tree, every year (Clark et al. 2007*b*). Both data sets are incomplete in space and time, with diameter measurements obtained for every tree and a subset of years, and tree-ring data available for a subset of trees, but every year up to the year in which the increment core was obtained. The credible intervals from that analysis closely follow the observations, with the widths determined by the number and type of observations and how they are distributed in time and among individuals (Fig. 5).

Like the diameter covariates, light availability was inferred based on the combination of three data types, synthesized with a hierarchical Bayes model. These three data types are summarized by a single variable name $C_{ij,t}$ in Fig. 3. Canopy status observations consist of an ordinal scale of 1, suppressed (no crown exposed to direct sunlight); 2, intermediate (less than 20% of crown exposed to direct sunlight); and 3, codominant (>20% canopy exposure). Remotely sensed canopy area was the second data type, including measurement of canopy exposed to direct sunlight from low-altitude digital video. The third "data type" involved shade indices based on heights and distances of each individual's neighbors. As with diameter covariates, the posterior precisions for light availability depend on all data types. The incorporation of priors for covariates is discussed in the next section.

Sample sizes are shown for tree scale data in Table 6 and for seed trap data in Table 7. Species vary in terms of the amount of each data type, but even for the more poorly represented species, the amount of information is substantial. For example, although we have only 68 individuals of *Carya ovata*, we have 694 tree years. We were particularly concerned with correlations between tree diameter D and canopy exposure λ and the need to include small trees subject to high light. Although not evident in the summaries of Table 6, we show that the combination of natural variation and canopy gap formation provides a broad range of covariate combinations. The model summarized in Fig. 3 includes submodels for each of data sets in Tables 6 and 7 and discussed here.

Seed data.—Seed data are modeled as in Clark et al. (2004), with a Poisson likelihood for seeds from all trees of the species to a given seed trap in year t (Fig. 4):

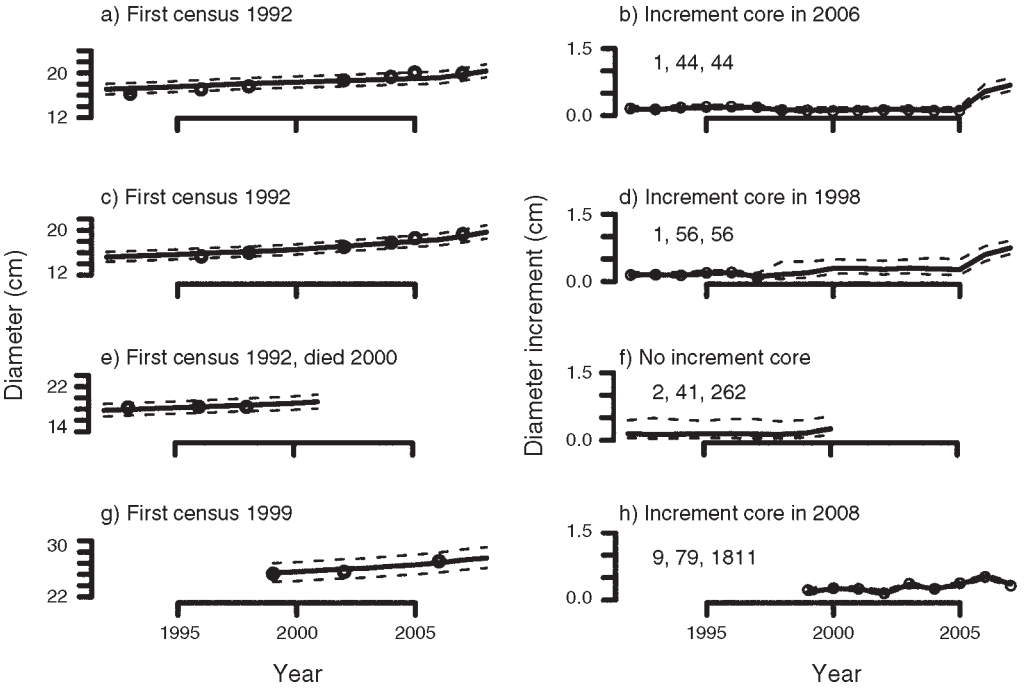

FIG. 5. Posterior densities for diameter $D_{ij,t}$ at left and diameter increment $d_{ij,t}$ at right, represented by median (solid line) and 95% credible intervals (dashed lines) compared with observations (dots). Series vary in length, depending on when observations began for the individual tree and its survival. Posterior densities are generally narrow where increment core data are available, and vice versa. Numbers at right indicate individual i, plot j, and a unique order number in the database). These densities are used as priors for each tree year in the analysis discussed here. This example is for *Quercus*, based on the analysis of Clark et al. (2007*b*).

$$\prod_k \text{Pois}(s_{jk,t} \mid g_{ijk,t}). \tag{1}$$

Let $\mathbf{g}_{j,t} = [g_{j1,t}, \ldots, g_{jK,t}]$ be the vector of expected seed intensities for each seed trap in stand j, year t. Then,

$$\mathbf{g}_{j,t} = \mathbf{A}_j(\mathbf{1}_K cB_j + \mathbf{F}_{j,t}\mathbf{f}_{j,t}) \tag{2}$$

where $\mathbf{A}_j$ is the vector of seed trap areas A_{jk} (m^2), c is a fitted parameter, B_j is the basal area of the species in stand j, $\mathbf{1}_K$ is length-K_j vector of ones, $\mathbf{F}_{j,t}$ is the K_j by $n_{j,t}$ matrix of dispersal kernel values, and $\mathbf{f}_{j,t}$ is the length $n_{j,t}$ vector of fecundities, where $n_{j,t} = \Sigma_i Q_{ij,t}$ is the number of fecund trees in stand j in year t. The first term allows that seed may come from outside the mapped plot and is taken to be proportional to basal area for the species, with fitted parameter c. The second term is source strength, a vector of fecundities $\mathbf{f}_{ij,t}$ multiplied by the kernel with parameter u, a two-dimensional Student's t distribution, with element ijk being

$$F(r_{ijk}) = \frac{1}{\pi u(1 + r_{ijk}^2/u)^2} \tag{3}$$

for distance r_{ijk} (Clark et al. 1999, 2004). Thus, expected seed intensity depends on the latent state variables $\mathbf{f}$, discussed in *Synthetic model development*.

Maturation.—The probability of identifying the mature state is as follows:

$$p(q_{ij,t} = 1 \mid Q_{ij,t} = 1) = v \tag{4}$$

and failure to identify it is

$$p(q_{ij,t} = 0 \mid Q_{ij,t} = 1) = 1 - v.$$

There are no false positives, $p(q_{ij,t} = 1 \mid Q_{ij,t} = 0) = 0$. Because the transition cannot be directly observed, it is modeled as a hidden Markov process (*Synthetic model development*).

Survival.—The likelihood for survival status is

$$\text{Bernoulli}(z_{ij,t} \mid \zeta_{ij,t}) \tag{5}$$

where $z_{ij,t} = 1$ is the event that an individual survives, and $z_{ij,t} = 0$ if the individual dies. The survival probability $\zeta_{ij,t}$ depends on growth rate and size, discussed in *Synthetic model development*.

Synthetic model development

The process model assumes individuals are immature when small, growth occurs each year, and, with increasing size, trees make the transition to maturity, after which reproduction can occur. Each year growth accumulates with an associated risk of death. Diameter and diameter increment are both predictors and response variables, in the conditional sense: diameter growth in year t is one of the covariates for growth in year $t + 1$, as well as maturation and fecundity. A key feature of the process model is the assumption that

responses for trees in immature and mature states can differ, allowing for the fact that mature individuals must allocate to reproduction. We use techniques developed previously to model fecundity conditional on underlying status (Clark et al. 1998, 1999, 2004, LaDeau and Clark 2001, 2006) and extend them here to the joint growth/fecundity/survival response. Because fecundity inference is a goal, and seeds cannot be confidently identified to the species level, we model genera, with species differences within genera being specified by parameters (see Clark et al. 2004). Here we describe the joint modeling of demographic rates, which are the latent states that generate data (see *Data models*).

Juvenile growth.—Immature trees grow and are subject to mortality risk, but they do not produce seed. Diameter growth for tree i of species h in stand j and year t is delineated by

$$\ln d_{hij,t} = \mathbf{x}_{hij,t-1}\mathbf{a}_h + b_{hr,t} + b_{hij} + w_{hij,t} \tag{6a}$$

$$w_{hij,t} \sim \mathcal{N}(0, \sigma^2) \tag{6b}$$

$$b_{hij} \sim \mathcal{N}(0, v_b) \tag{6c}$$

where $d_{ij,t}$ is the diameter increment (cm) from year $t-1$ to year t:

$$\mathbf{x}_{hij,t-1} = [\,1 \quad \ln D_{hij,t-1} \quad \ln^2 D_{hij,t-1} \quad \ln \lambda_{hij,t-1} \quad \ln d_{hij,t-1}\,] \tag{6d}$$

is the design vector for intercept, log diameter, log diameter squared, log ECA, and the lag-1 term, respectively, $\mathbf{a}_h$ is the corresponding vector of fixed effects parameters for species h, b_{hij} is a random individual effect, $b_{hr,t}$ are fixed year effects for year t in region r, and $w_{hij,t}$ is the process error. Within a region, the year effects sum to zero, so they represent departures from the overall mean. Elements of $\mathbf{x}_{ij,t}$ are estimates and thus updated in the model as well (Appendix A). There are three sets of fixed year effects $r \in \{1, 2, 3\}$ one each for the Blue Ridge (C), Transition (M), and the Piedmont (D; Table 3). Year effects capture interannual variation on a regional scale, such as that related to climate variation and masting. We use three sets of year effects, not only because year effects could differ between regions, but also sampling began in different years. The full intercept is species intercept + year within region + individual effect (random) + year effect (zero sum).

Maturation.—As long as individuals remain immature, $Q_{hij,t} = 0$, Eq. 6 is used to describe growth. With increased size and light access individuals make the transition to the mature state $Q_{hij,t} = 1$. Let $\theta_{hij,t}$ be a latent state, the increasing probability of maturation with diameter $D_{hij,t}$ and exposed canopy area $\lambda_{hij,t}$. Then,

$$p(Q_{hij,t} = 1 \,|\, D_{hij,t}, \lambda_{hij,t}) = \theta_{hij,t} = \frac{\exp(\beta^\theta_{h0} + \beta^\theta_{h1} D_{hij,t} + \beta^\theta_{h2}\lambda_{hij,t})}{1 + \exp(\beta^\theta_{h0} + \beta^\theta_{h1} D_{hij,t} + \beta^\theta_{h2}\lambda_{hij,t})} \tag{7}$$

is a logit for the maturation probability. Thomas (1996) used a logit to model maturation with stem diameter. Our inclusion of canopy area recognizes that resources can affect maturation (LaDeau and Clark 2001, Clark et al. 2004). In the absence of observations, $\theta_{hij,t}$ is the probability that an individual of diameter $D_{hij,t-1}$ and exposed canopy area $\lambda_{hij,t}$ is mature. Observations change this probability, depending not only on the numbers of times that an individual is observed to be immature or not, but also on when those observations occurred. If there is a single year and observation, then probabilities given in Table 8 apply (Clark et al. 2004). Additional observations complicate the relationship. For example, maturation has lower probability in year t for an individual last observed to be immature in year $t-1$ than for an individual last observed to be immature in year $t-5$. Likewise, maturation has higher probability in year t for an individual first observed to be mature in year $t+2$ than for an individual first observed to be mature in year $t+10$.

For dioecious species, the probability of being female is $\phi = p(H = 1)$. Because an individual is only designated as male or female if certain, there are no false positive identifications associated with $h_{hij,t}$; however, most observations are "uncertain," $h_{hij,t} = 0$ (Table 8). The joint probabilities of maturation status and observations are detailed in Appendix A.

Mature growth and fecundity.—Once mature, seed production depends on covariates, including diameter, growth rate, and resources. There is some level of synchronicity among individuals due to masting, climate variation, or both, and there are individual differences beyond those accounted for by covariates. There is error in the model itself. Because both diameter growth and fecundity are response variables, we include them together as a multivariate regression within the state–space model. This approach allows us to explicitly include error covariance between growth and fecundity beyond that which is accommodated by covariates. Let

$$\mathbf{y}_{hij,t} = [\,\ln d_{hij,t} \quad \ln f_{hij,t}\,] \tag{8a}$$

be the response vector consisting of ln(diameter increment) (measured in centimeters) and ln(fecundity) (seed production potential). The response is modeled as

$$\underset{(1\times 2)}{\mathbf{y}_{hij,t+1}} = \underset{(1\times p)}{\mathbf{x}_{hij,t}}\,\underset{(p\times 2)}{\mathbf{A}_h} + \underset{(1\times 2)}{\mathbf{b}_{r,t}} + \underset{(1\times 2)}{\mathbf{b}_{hij}} + \underset{(1\times 2)}{\boldsymbol{\varepsilon}_{hij,t}} \tag{8b}$$

$$\mathbf{b}_{hij} \sim \mathcal{N}_2(\mathbf{0}, \mathbf{V}_b) \tag{8c}$$

$$\boldsymbol{\varepsilon}_{hij,t} \sim \mathcal{N}_2(\mathbf{0}, \boldsymbol{\Sigma}) \tag{8d}$$

where $\mathbf{x}_{hij,t}$ is a design vector (Eq. 6d), $\mathbf{A}_h$ is matrix of fixed effects parameters, $\mathbf{b}_{r,t}$ are fixed year effects, $\mathbf{b}_{hij}$ are random intercepts with covariance $\mathbf{V}_b$, $\boldsymbol{\varepsilon}_{hij,t}$ is the vector of errors, and $\boldsymbol{\Sigma}$ is the 2×2 covariance matrix. As with juvenile growth, there is a sum-to-zero constraint on $\mathbf{b}_{r,t}$ over years, for each r. This amounts to a state space model in which diameter increment (and, thus, diameter)

is both a predictor and a response, being updated each year. Together, this represents a minimal model with effects of size and resources (in this case, light availability) on reproduction and growth. This design matrix can accommodate additional main effects and interactions (J. S. Clark, D. M. Bell, M. H. Hersh, and L. Nichols, *unpublished manuscript*).

The rows of $\mathbf{A}_h$ (Eq. 8b) correspond to the elements in $\mathbf{x}_{hij,t-1}$ (Eq. 6d). The columns of $\mathbf{A}_h$ correspond to the elements of $\mathbf{y}_{hij,t}$ (Eq. 8a). An example of $\mathbf{A}_h$ is shown here, with labels for rows (predictors) and columns (responses):

$$\begin{array}{l} \\ \text{intercept} \\ \ln D_{t-1} \\ \ln^2 D_{t-1} \\ \ln \lambda_{t-1} \\ \ln d_{t-1} \end{array} \begin{array}{c} \begin{array}{cc} \ln d_t & \ln f_t \end{array} \\ \begin{bmatrix} A_{11} & A_{12} \\ A_{21} & A_{22} \\ A_{31} & A_{32} \\ A_{41} & A_{42} \\ A_{51} & A_{52} \end{bmatrix} \end{array}. \tag{8e}$$

Of course, year effects could have been included in $\mathbf{A}_h$; we sampled them separately to isolate the overall intercept in $\mathbf{A}_h$ and impose a sum-to-zero constraint on year effects (Appendix A).

With recent attention on spatial random effects (e.g., Banerjee et al. 2006), one could question why this explicitly spatial model includes random effects that are non-spatial (Eqs. 6c, 8b). The capacity to model spatial correlation in random effects is important where the role of space cannot be captured in the portion of the model describing processes. For example, individual growth rates could be either positively or negatively correlated with those of neighbors, because they share the same high (or low) resource patch or growth of one suppresses growth of another. More powerful and informative than spatial random effects is to actually measure (or estimate directly) the process that would produce such correlations. At the scale of individual growth, the resource that varies and most strongly affects growth is light availability. By making light effects explicit, we learn about them directly, rather than attempting to interpret them from a spatial covariance matrix. It is straightforward to demonstrate that spatial random effects are not needed here, by inspection of the correlations between individual random effects with distance. We find no such distance trend (Appendix A). The lack of trend does not mean that growth rates are uncorrelated. On the contrary, individuals are responding to many of the same variables. Rather, once the factors that cause correlation are taken up in the process model (in this case, light availability), there is no residual correlation.

Survival.—Due to inadequacy of parametric survival forms, we implemented the survival model of Clark et al. (2007*a*, see also Metcalf et al. 2009, Vieilledent et al. 2009), which extends the nonparametric survival model of Wyckoff and Clark (2000). Mortality risk declines with tree vigor, which tends to be lowest in the small trees that grow slowly in the shaded understory and for large trees as they approach senescence (e.g., Platt et al. 1988, Uriarte et al. 2004). Thus, mortality risk both decreases and increases with tree size, but for different reasons. Our approach distinguishes effects of tree vigor and tree size. The survival model is nonparametric, allowing increase in mortality risk with decreasing growth rate (a composite index of vigor; Kobe 1996, Wyckoff and Clark 2000) and with increasing diameter (Platt et al. 1988, Batista et al. 1998, Uriarte et al. 2004) and strong nonlinearities in these relationships. We impose only a monotonicity constraint, which is less rigid than parametric models that assume not only monotonicity, but also a specific functional form. In the Bayesian implementation used here, monotonicity is part of the prior specification. In the Clark et al. (2007*a*) model (see also Metcalf et al. 2009*a*), each individual in each year has a pair of risks (μ_{hd}, μ_{hD}) associated with growth rate (monotonically decreasing) and diameter (monotonically increasing), with survival probability from year $t-1$ to year t being

$$\zeta_{hij,t} = 1 - (\mu_{hd} + \mu_{hD} - \mu_{hd}\mu_{hD}). \tag{9}$$

Latent states.—Each of the foregoing submodels includes explicit state variables, including diameter $D_{hij,t}$, diameter increment $d_{hij,t}$, canopy area $\lambda_{hij,t}$, fecundity potential $f_{hij,t}$, maturation status $Q_{hij,t}$, gender H_{hij}, survival probability $\zeta_{hij,t}$, and maturation probability $\theta_{hij,t}$ (Fig. 3). Two of these variables are deterministic transformations of other modeled variables and thus do not need to be modeled themselves. This includes survival probability $\zeta_{hij,t}$ and maturation probability $\theta_{hij,t}$: we can simply evaluate them using Eqs. 9 and 7b, respectively. Others are both predictors and responses and are modeled with uncertainty, including $d_{hij,t}$, $\lambda_{hij,t}$, $f_{hij,t}$, $Q_{hij,t}$, and H_{hij}. These are modeled together with parameters based on the conditional relationships in this section and data models of the previous section (Appendix A).

Prior distributions

The analysis includes both informative and non-informative prior distributions. Where possible, we used informative prior distributions that are flat but truncated reflecting natural limits, to maximize transparency, i.e., for clear identification of the contributions of prior vs. likelihood. In Appendix A, we provide a detailed summary of prior distributions and how they were selected to balance information.

Computation

The posterior distribution was simulated with Metropolis-within-Gibbs, based on conditional posteriors that are discussed in Appendix A. The simulation was initialized at prior mean values (diameter increments and crown areas), random draws from priors, or inversion of models based on priors (fecundities). Extended chains of all parameters were examined, as were samples of large numbers of latent variables. Note

that, with the exception of random effects in growth and fecundity, all variance parameters are given informative priors, to insure effective mixing and convergence (Natarajan and McCulloch 1998, Dunson 2009). Despite complexity, rapid convergence is facilitated by several features of the algorithm, including integrating out random effects in the sampling of fixed effects, an initialization of fecundities that is informed by the process model, and an adaptive sampling scheme, not only in terms of proposal size, but also alternately drawing from likelihoods based on the process and data sets. All computational details are included in Appendix A.

Model Evaluation

The evaluation of large models is challenging, particularly with an increasing reliance on information criteria as one of the few widely reported diagnostics. Information criteria do not provide much guidance for evaluation of models, and essentially none for large models. Criteria such as Akaike information criterion (AIC), Bayesian information criterion (BIC), and deviance information criterion (DIC) are used to compare the fits of two different models to the same data set. They consist of a goodness-of-fit term and a "penalty" term for model size. For situations where multiple models can and should be compared and selected on the basis of their fit to a single data set, these metrics based on deviance are worth consultation. There are many situations where model selection should not be based on a single number, even when models are small enough to make such numbers interpretable (Clark et al. 2004, Link and Barker 2006, Clark 2007). Outside ecology such criteria do not play such a large role (e.g., Gelman and Hill [2007] mention deviance-based criteria only briefly, suggest caution, and dismiss the low-DIC model in their single example). Many models are built to represent known phenomena in parsimonious ways, not provide the best fit to a particular data set. For example, general circulation models of the atmosphere and numerical weather prediction models (Gel et al. 2004) are not selected based on information criteria. In our case, the model is limited to known phenomena; we include variation and uncertainty at several scales, not because it might improve the fit, but rather to provide a more comprehensive description. Maximizing the fit to any one data set (i.e., the rationale for model selection by information criteria) is not the point; rather we are interested in combining their contributions, consciously sacrificing the fit to any one in the interest of synthesis. Moreover, for large models, the penalty for model size becomes arbitrary. The number of parameters in a hierarchical model cannot be objectively determined, and calculations of "effective parameters" (Spiegelhalter et al. 2002) yield erratic results. The most important point here is that information criteria for comparing fits of different models to a data set is not the same as model evaluation, which involves a larger set of issues.

Large models can suffer from a range of problems, involving the underlying model, computation, and the specific data sets (Geweke 2004, Cressie et al. 2009), which information criteria do not address. Model structure may not permit effective identifiability of parameters (do data provide information on all parameters in the model?) or it may contain errors in logic (mathematics). Computational issues involve construction of the Markov chain Monte Carlo model (MCMC; can it efficiently explore the posterior?) and evaluation of its behavior (has it converged?). Finally, determining the extent to which the posterior distribution is informed by different data sets and the prior is crucial to interpreting output.

Simulation is one of the most powerful tools for model evaluation (e.g., Gelman and Hill 2007, Clark and Hersh 2009; Scott and Berger, *in press*), used to (1) generate data sets from known parameters, which are then compared with estimates from the model, and (2) generate data sets from estimated parameters, which are then compared with actual data. The first option is not always practical for large models (Clark and Hersh [2009] provide an example for a large network of species interactions). The current application could not be feasibly evaluated in this way. We made extensive use of the second option, comparing predictive distributions of data with observation from data used to fit the model and external data. Here we illustrate how predictions from different levels of the model can help can elucidate the role of uncertainty at different levels in the model. We supplement these results with prior/posterior comparisons posterior summaries that provide evidence of identifiability.

Not reported here is extensive experimentation, beginning with submodels in isolation and individual data sets, progressively stepping up to the full analyses of all sites and components operating together. We agree with the recommendations of Craigmile et al. (2009) that components of large models need independent evaluation. We have done this for fecundity (Clark et al. 2004), diameter growth (Clark et al. 2007*b*, Metcalf et al. 2009*b*), and mortality (Clark et al. 2007*a*, Metcalf et al. 2009*a*, Vieilledent et al. 2009).

Distribution of data

To confirm that experimental manipulations provided a full range of covariates, particularly for tree size and canopy exposure, we begin with this distribution. Because of the large number of gaps in the canopy followed over a number years (Fig. 2), we obtained good representation of small individuals receiving high light as well as other canopy area/diameter combinations (Fig. 6). This 17-year study of 11 different stands provides a broad range of light levels and tree sizes for a large number of species. Experimental gap creation helps break up the correlation between tree size and light

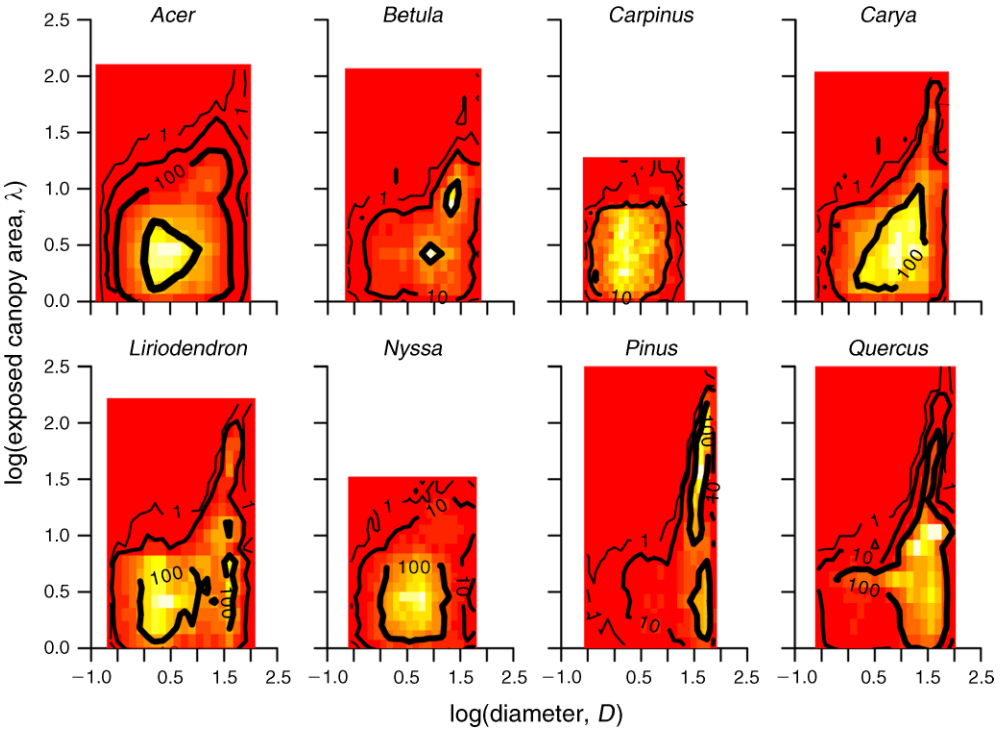

FIG. 6. Numbers of observations plotted against diameter and exposed canopy area, showing coverage of covariates that predict growth and fecundity. With the exception of the largest trees, there is substantial representation of observations from small trees with high light and vice versa. High values are yellow, low values are red, and contours are 1, 10, 100, and 1000.

availability. Although there is positive correlation for the largest trees, with large individuals tending to receive more light, we have many small individuals in high light environments (Fig. 6). Moreover, due to the intervention design, light is not redundant with individual effects: if individuals remained in approximately the same light environment throughout the study, it would be difficult to separate the two. In this study, we have many individuals in different light conditions, with sufficient time to respond.

Parameter correlations

Strong correlation in parameter estimates can be undesirable, sometimes indicating a weak capacity to identify parameters and potential for inadequate mixing of the MCMC. That does not mean that latent variables should be uncorrelated; indeed quantifying such relationships is a goal of the analysis. Rather, we wish to determine if some of the parameters are highly correlated as indication of limited identifiability. We did extensive analysis of posteriors, Fig. 7 showing an example of correlation structure. Of 133 principle parameters, involving $133 \times 132/2 = 8778$ comparisons, only a few have absolute value exceeding 0.5, and most of these involve the monotonic sequence of mortality bins. The positive correlations for elements of μ_d come from the fact that they are sequential elements of a series and must covary. Likewise, correlations in year effects $\mathbf{b}_{r,t}$ are expected when there is masting and persistent effects of variation on demography. Despite the large number of parameters only a few show even intermediate levels of correlation.

Prior/posterior comparisons

To determine the extent to which estimates depend on prior densities vs. other information entering the model, we compared prior and posterior densities. A posterior distribution that does not differ from the prior indicates that the analysis has not updated prior knowledge. Alternatively, large differences indicate "disagreement." A full summary in provided in Appendix A.

Fig. 8 illustrates contributions of prior and data to posterior and predictive distributions for maturation and gender for *Acer*, which includes both monoecious (*A. barbatum*, *A. saccharum*) and dioecious (*A. rubrum*, *A. pensylvanicum*) species. In fact, *A. rubrum* is polygamo-dioecious, having some individuals that are male, some female, and some supporting both male and female flowers. The estimate of female fraction for this genus includes both female and monoecious individuals. The marginal posteriors for the parameter vector $\boldsymbol{\beta}^{\theta}$ (Fig. 8a) are narrow and they differ from the prior (flat green lines). The positive estimates for diameter and canopy area indicate increasing maturation probability with these covariates.

The estimates for the population-level maturation relationship are given by predictions of θ. These are plotted against exposed canopy area λ (for two values of diameter in Fig. 8b) and against diameter D (for the mean canopy area). The estimates of $\boldsymbol{\beta}^{\theta}$ predict the population-level relationship for θ (smooth black lines in Fig. 8b, c). The black histograms in Fig. 8b, c summarize individual-level estimates. The population-level predictions do not appear to run precisely through the histograms of individual-level predictions, because the individual-level predictions effectively marginalize over diameter and canopy distributions for the entire population, whereas the predictive mean curves are conditional on the specific diameter and canopy values. Note that the predictions for two values of λ lie above and below the histogram of individual level estimates in Fig. 8b.

With increasing diameter and canopy area, larger numbers of individuals are observed to be mature (red histogram in Fig. 8b, c) and still more are estimated to be mature (black histogram), because detection is uncertain (horizontal dashed red lines). Note that the posterior 95% credible interval for the estimate of $\nu\phi$ is the expected fraction identified when trees are large enough to all be mature. The 95% credible interval (dashed red) roughly averages the red histogram of observations. In contrast, the black histogram of estimates approaches 1. This is the expected relationship between observations, detection probability, and the true states. The values approach zero for small diameters (Fig. 8c), because small trees cannot reproduce. However, values do not approach zero for small exposed canopy areas (Fig. 8b), because it is possible for trees that are highly shaded to yield at least some fruit, in most cases when they are large.

Gender inference improves with tree size, because large trees are more likely to be reproductive, and reproduction is the only evidence for gender. Of the four species included in the analysis of *Acer*, two include males (*A. rubrum*, *A. pennsylvanicum*). Gender observations are "unknown" for most, particularly individuals in the smallest size classes. At small diameters, there many estimates at zero, one, and the mean estimate of φ (Fig. 8e). Those estimated near zero (male) at small size represent individuals that will grow sufficiently large during the study to eventually have information suggesting lack of reproduction, despite being of a size where maturation probability is high. Those estimated near one (female) at small size represent individuals of a dioecious species that will later show evidence of reproduction, thus providing evidence that they were female throughout, and all individuals of the monoecious *A. barbatum* and *A. saccharum*. Those clustered near the posterior mean of φ never have strong evidence of reproduction or not and thus remain uncertain. This includes individuals who are small throughout or are large but far from seed traps, thus having little evidence of reproductive status. Estimated probability of being female tends to zero or one with increasing diameter (Fig. 8d). With increasing confidence in maturation status, we see a greater tendency to be female than to be male (Fig. 8e). This tendency results from the fact that two of the species in *Acer* are monoecious and thus are included in female class, regardless of maturation status or size.

The influence of truncated priors (Appendix A) on estimates for the state space component of the model (Eq. 8) is evident in posteriors for parameters from the growth/fecundity state-space model (Fig. 9). Fig. 9 is organized in rows and columns to match the structure of parameter matrix $\mathbf{A}_h$ (Eq. 9e). Finding strong effects of truncation points on posteriors is not undesirable: the flat, truncated priors provide transparency, i.e., clear distinction between contribution of prior and likelihood. In light of the size and complexity of the model the flexibility to assign hard boundaries to one or both limits for these parameters and the transparency of prior effects on posteriors was deemed an advantage. For this example, we held the diameter effect D on growth rate d (parameter A_{21}) to be near zero (there is no prior knowledge to suggest growth rate should respond directly to size until trees become large), but assumed that the effect of D on fecundity (parameter A_{22}) should fall between 1.5 and 3.5 (*Prior parameter values*). Together these assumptions allow for a direct size effect on fecundity that accords with allometric theory. Thus, we allow for the fact that size is correlated with fecundity, but that the effect of exposed canopy area depends on allometry.

To allow for declining growth and fecundity with size, we included the $\ln^2 D$ term in the model (parameter A_{31}) and constrained it to be negative. This term has increasing influence with size. We did not have enough large enough trees for all species to show clear effects of large size on growth (posteriors truncated at the upper zero boundary), but there was evidence for this negative effect on fecundity for a number of species. Canopy exposure λ has a positive effect on both growth and fecundity (A_{41}, A_{42}).

The lagged growth rate effect was constrained to be near zero for growth (parameter A_{51}), because we wanted long-term trends in growth to be taken up by year effects; the tendency for positive correlation in this examples was constrained by the upper boundary at 0.01. However, we wanted to explicitly parameterize the lag-1 effect of growth on fecundity (parameter A_{52}), because this could be important for demographic prediction. We obtained a range of values from strongly positive to strongly negative for the lag-1 effect of growth on fecundity; for this example (Fig. 9) it is negative.

Taken together, Fig. 9 illustrates the combined contributions of prior and data. Clearly priors define some hard and transparent limits that conform to known relationships. On the other hand, posteriors deviate substantially from the priors indicating the

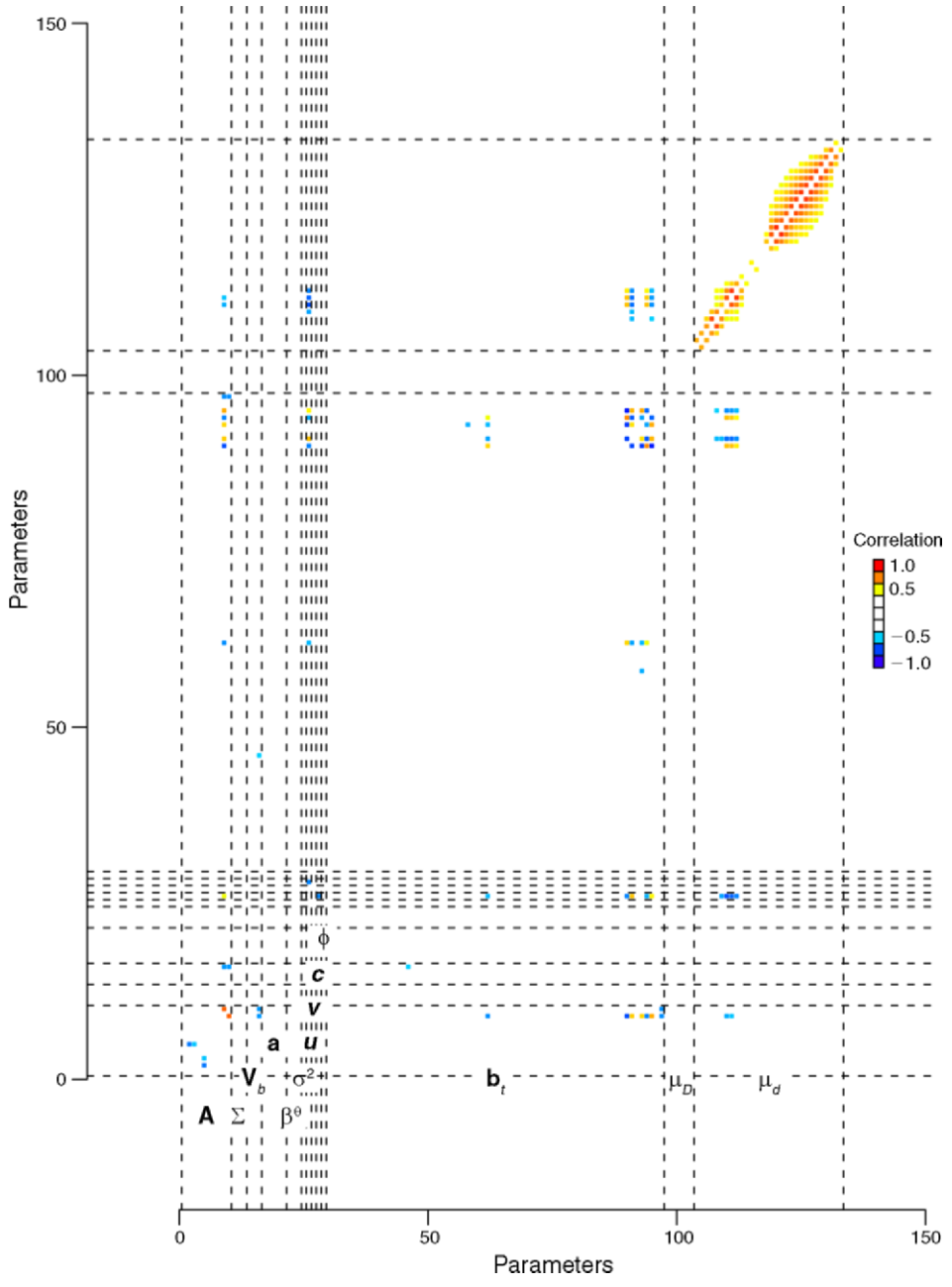

FIG. 7. Correlations between estimates of population parameters for *Fraxinus*. Low correlations (between −0.5 and 0.5) are omitted for clarity. Parameter names indicate fixed effects on adult growth and fecundity (**A**, Eqs. 8b and A.4), process error covariance matrix on growth and fecundity (**Σ**, Eqs. 8d and A.5), fixed effects on juvenile growth (**a**, Eq. 6a), random effects covariance matrix ($\mathbf{V}_b$, Eqs. 8c and A.6), maturation probability (β^θ, Eqs. 7 and A.1), juvenile growth process error variance (σ^2, Eq. 6b), dispersal (u, Eqs. 3 and A.11), maturity recognition (v, Eqs. 4 and A.2), out-of-plot fecundity contribution (c, Eqs. 2 and A.11), female fraction (ϕ, Eq. A.3), year effects on growth and fecundity ($\mathbf{b}_t$, Eqs. 8b and A.7), diameter effect on survival (μ_D, Eq. 9), and growth rate effect on survival (μ_d, Eq. 9). Note that Eqs. A.1–A.11 are in Appendix A.

strong contribution of data. The transparency of truncated priors provides an important input, without sacrificing transparency or the role of data away from boundaries.

Fixed-year effects for the state–space model summarize year-to-year variation that is not taken up by covariates and shared among individuals. There are substantial differences between the three regions (Fig. 10). Those for Coweeta (black curves) extend back to 1992, whereas those for the Piedmont (green curves) and Mars Hill (red curves) begin in 1999 and 2004, respectively. Those for fecundity show a tendency for

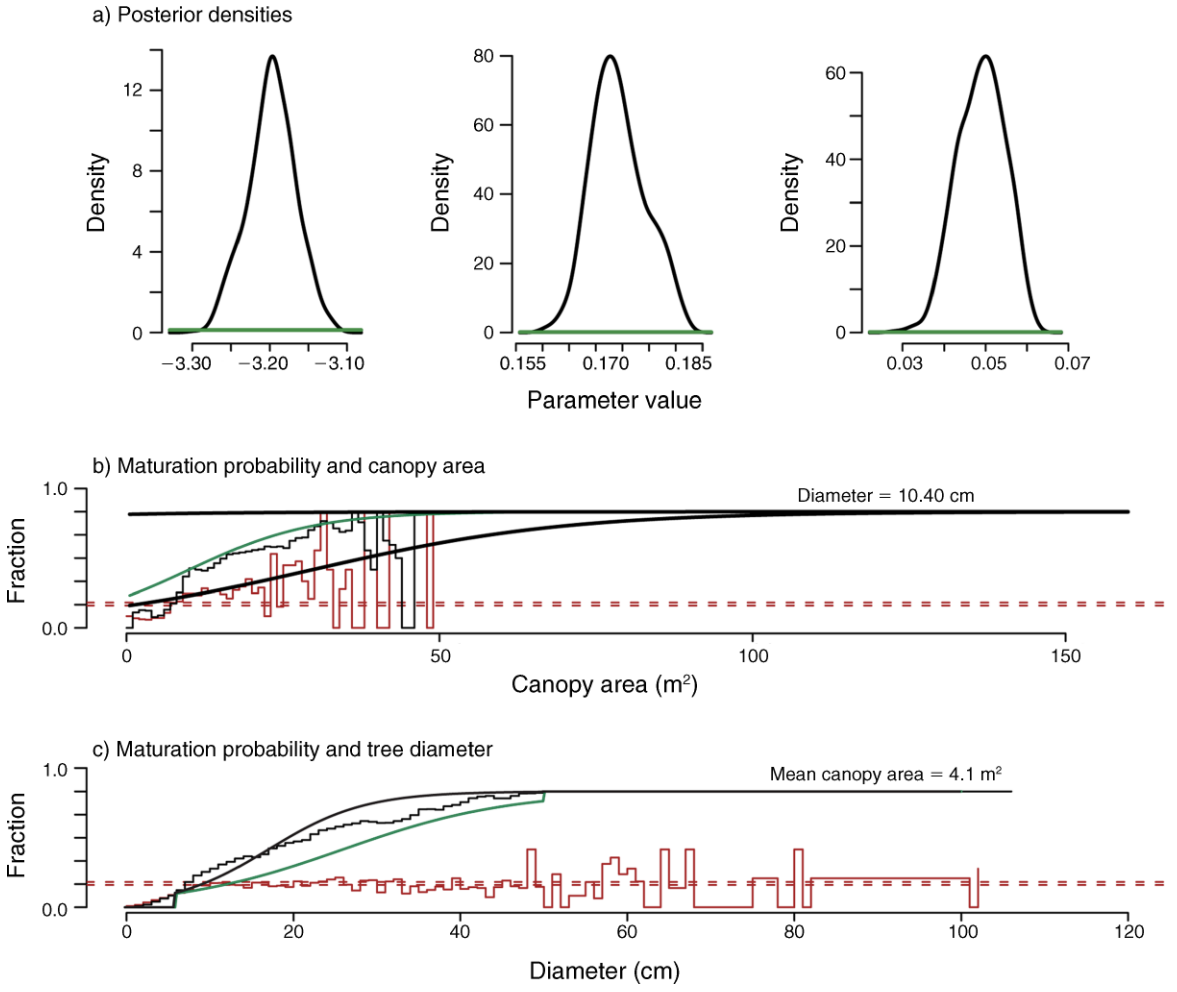

FIG. 8. Data and fitted models for maturation and gender for *Acer*. (a) Posterior (black) and prior (green) densities are shown for the maturation parameters β^{θ} (Eq. 7). (b, c) Red histograms show the fraction of observations in diameter bins and exposed canopy area bins, respectively, recognized as mature, i.e., for which $q_{ij,t} = 1$. Black histograms show the fraction estimated to be mature, i.e., those for which the estimates $Q_{ij,t} = 1$. The function θ is shown for prior (green) and posterior (black) mean values of β^{θ}. Horizontal dashed lines (red) are 95% CIs for $\nu\phi$, the probability of being both female and recognized as mature. (d, e) Circles show posterior means for gender plotted against (d) diameter and against (e) posterior mean maturation probability.

2–5 year mast cycles in some taxa (e.g., *Fraxinus*), but not in others (e.g., *Liriodendron*). The regional differences are large and partly resulting from climate differences (J. S. Clark, D. M. Bala, H. H. Hersh, and L. Nichols, *unpublished manuscript*).

The posterior estimates for effects of diameter increment μ_d and diameter μ_D on survival show the flexibility of the monotonicity assumptions (Fig. 11). The relationship between growth increment and mortality risk is highly nonlinear near the lowest growth rates (Fig. 11a, b). Apparently, trees reach a threshold of low growth, below which mortality risk rises substantially. The histogram of diameters when trees died in Fig. 11c shows modes not only at the largest diameters, but also the smallest. The latter mode results from the slow growth at low light levels in the forest understory. The priors help to discriminate the growth from size effects, by recognizing that mortality risk declines with growth rate (Fig. 11b), but increases with size (Fig. 11c). Beyond this relationship already known from previous studies, the prior does not prescribe the shapes of these relationships. The positive correlations in estimates observed for μ_d parameters (Fig. 7) result from monotonicity.

Extensive comparisons of priors, observations, and posteriors as summarized in Figs. 6–11 helped us evaluate the model, assuring that estimates are sensible and provide insight on contributions from observations and priors. The latent states diameter growth, maturation status, fecundity, and mortality risk are unobserved but can be evaluated in more indirect ways that are summarized in the next section.

Diagnostics involving latent state prediction

To provide further insight into model behavior we predicted data and compared predictions with posterior

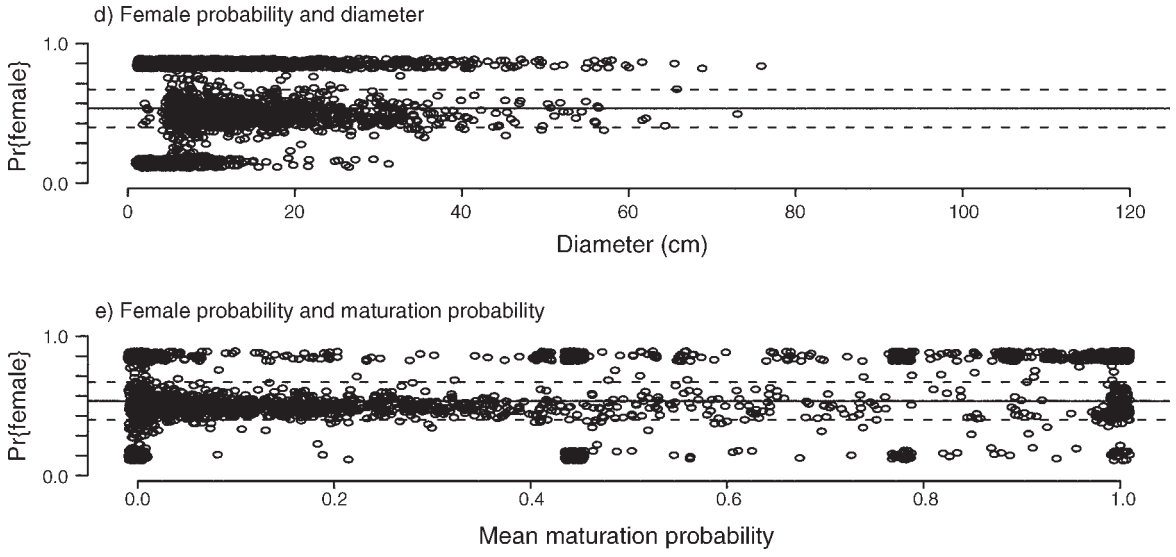

FIG. 8. Continued.

estimates of latent states and with observations. Predictive distributions have the general form

$$p(R \mid \mathbf{X}^*, \mathbf{X}) = \int p(R \mid \mathbf{X}^*, \boldsymbol{\pi}) p(\boldsymbol{\pi} \mid \mathbf{X}) d\boldsymbol{\pi}$$

where $\mathbf{X}$ is taken to be all data and priors entering the model, $\boldsymbol{\pi}$ is a vector of parameters, and $\mathbf{X}^*$ is taken to be values for a scenario of $\mathbf{X}$, i.e., those for which response R is to be predicted. $\mathbf{X}$ could apply to a spatial prediction grid, years in the past or the future, or covariate values other than those for which data were collected (Clark 2007). The integrand contains two factors, the likelihood structure and posterior, respectively. Predictive distributions are widely used to evaluate model fit, examples including cross validation and predictive loss (Gelfand and Ghosh 1998, Clark et al. 2004, 2007*b*, Gelman and Hill 2007). Here we describe some of these predictions and how they compare to data or estimates of latent states.

Predictions of diameter growth were evaluated against an independent data set of growth, obtained from measurements of increment cores spanning decades. These data were not used to fit the model. We initialized the model and incremented year-by-year predictive distributions, approximating $p(d_{t+1} \mid \mathbf{X}_t^*, \mathbf{X}) = \int p(d_{t+1} \mid \mathbf{X}_t^*, \boldsymbol{\pi}) p(\boldsymbol{\pi} \mid \mathbf{X})\, d\boldsymbol{\pi}$, where $\mathbf{X}$ is taken to be all data and priors entering the model, and $\mathbf{X}_t^*$ is the previously predicted diameter and increment and the distribution of canopy exposure values $\lambda_{ij,t}$ contained in the data. The integrand includes the state–space structure of the model (Eqs. 6, 7, 8) and the posterior, respectively. The integral is approximated by drawing at random a row from the iteration-by-parameter matrix of MCMC output. The tree is initially immature (1 cm diameter) and subject to the growth rate in Eq. 6, probability of maturation from Eq. 7, and risk of death from Eq. 9. $\mathbf{V}_b$ determines the random individual effect. The year effects are drawn at random from those included in the study (they are part of the iteration-by-parameter matrix of output). If the individual does not survive, it is removed from the simulation. If it survives, a Bernoulli trial with probability from Eq. 7 determines the new maturation status. The next growth rate is drawn from a univariate (Eq. 6) or bivariate normal (Eq. 8) distribution, depending on maturation status. The example in Fig. 12 is typical: we obtain good coverage of size distributions for century-ahead prediction. Note that the model contains no explicit age information. And there is no attractor in the model that would necessarily make it converge to a particular diameter value. Moreover, these are not one-step ahead predictions, as is often used to evaluate fits of time series models, but rather 200-year-ahead predictions.

A similar approach to prediction was used to evaluate other aspects of the model. Maturation status is partially known, and fecundity is not observed, so we cannot directly compare observations against model predictions. However, we can extend the approach for diameter growth to maturation status, comparing estimates of maturation statuses of individual trees plotted against their ages (not used to fit the model) with the predictive mean distribution of maturation ages based on the posterior distribution. This approach differs from Fig. 8, where we show comparisons of maturation involving tree size. Fig. 13 shows examples of estimates (dots) plotted against with the predictive means from the fitted model (smooth curves). The important point here is that predictions are close to individual estimates.

For fecundity, we evaluate predictions of seed rain. We did this in two ways. Consider that seed rain can be predicted from different levels in the model. The model

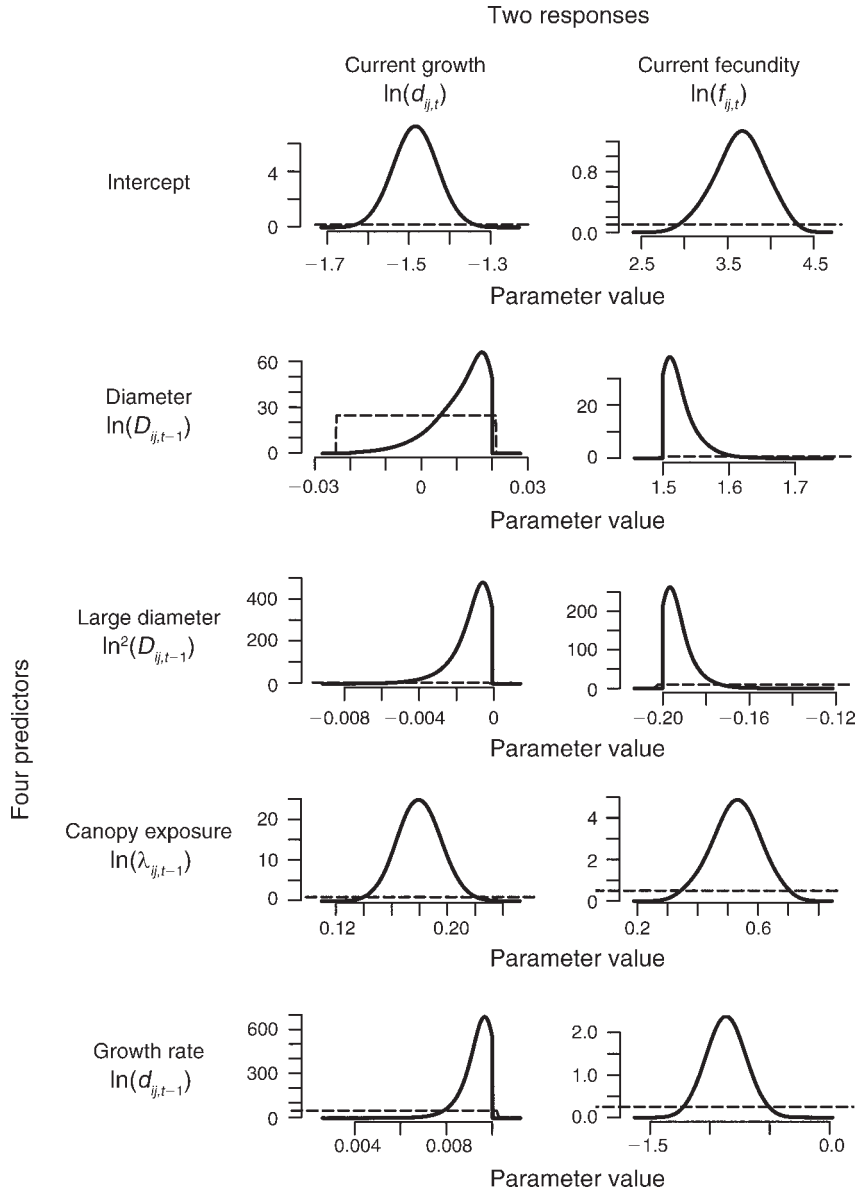

FIG. 9. Comparison of priors (dashed lines) and posteriors (solid lines) for the fixed effects in the parameter matrix **A** for the state space model (Eq. 4) for *Liriodendron*. The layout of plots matches Eq. 8e.

generates estimates of latent states $f_{ij,t}$, which balance information coming from seed rain data (Eqs. 1 and 2) and the model covariates (Eq. 8). Trees close to seed traps are heavily influenced by seed trap data (the kernel is a weighting function). Standard errors for the fecundity estimates for these trees are small (Fig. 4b). Fecundity estimates for trees distant from seed traps obtain most of their information from the model covariates and have higher uncertainty (Fig. 4c). Uncertainty increases as the number of mature trees greatly exceeds the number of seed traps. Note that when the number of seed traps exceeds the number of trees we can solve Eq. 2 directly (Appendix A). As the number of mature trees becomes large there are increasingly more ways to satisfy a set of seed trap observations, so standard errors will increase. Predictive intervals help to evaluate the consequences of this uncertainty. Based on these latent states for all trees in plot j in year t, there is a likelihood for seed rain data at location k in year t (Eqs. 1–3). Thus we can consider how well the expected seed production for all trees at j in year t predict seed rain observations at seed trap k in year t, or $p(s_{k,t} \mid E[\mathbf{f}_{j,t}, \mathbf{Q}_{j,t}], \mathbf{X}) = \int p(s_{k,t} \mid E[\mathbf{f}_{j,t}, \mathbf{Q}_{j,t}], u)p(u \mid \mathbf{X})\, du$, where $\mathbf{X}$ represents all data and priors, the first factor in the integrand is the Poisson likelihood (Eqs. 1 and 3) and the second is the marginal posterior for u. This prediction is conditioned on fecundity estimates. Alternatively, we could predict from a lower

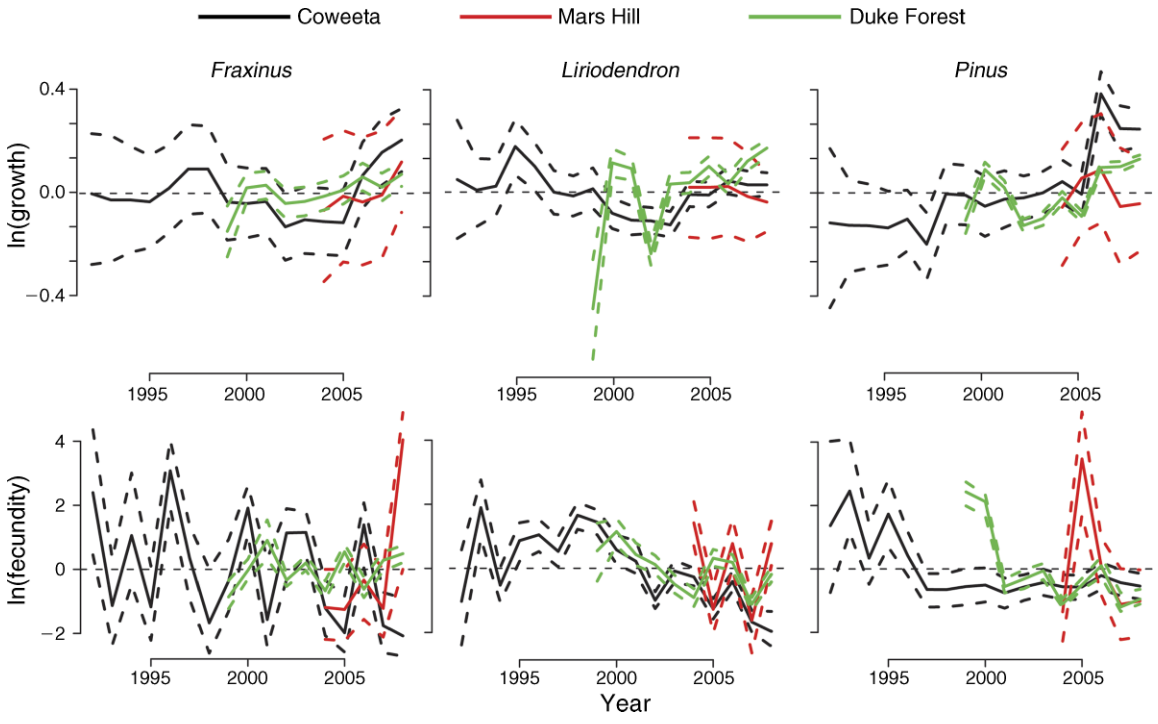

FIG. 10. Posterior medians and 95% CIs for year effects $\mathbf{b}_t$ (Eq. 8b) for three species in the three regions. Separate year effects were used for Blue Ridge (black), Mars Hill (red), and Piedmont (green). Note the scale difference: the range for fecundity is four times that for diameter growth.

level to include the uncertainty in $(Q_{ijt}, f_{j,t})$ and in the covariates $\mathbf{X}$:

$$p(s_{k,t}\,|\,\mathbf{X}) = \int p(s_{k,t}\,|\,\mathbf{f}_{j,t}, \mathbf{Q}_{j,t}, u)p(\mathbf{f}_{j,t}, \mathbf{Q}_{j,t}\,|\,\mathbf{X}', \boldsymbol{\pi}) \times p(\mathbf{X}', u, \boldsymbol{\pi}\,|\,\mathbf{X})\; d(\mathbf{f}_{j,t}, \mathbf{Q}_{j,t}, u, \boldsymbol{\pi}, \mathbf{X}')$$

where $\mathbf{X}'$ represents the estimates for diameter, diameter growth rate, and exposed canopy area, and the vector $\boldsymbol{\pi} = (\mathbf{A}, \{\mathbf{b}_{r,t}\}, \{\mathbf{b}_{ij}\}, \Sigma)$.

Fig. 14 compares predictions from these two levels with data (black) and for missing data (red), where the horizontal axis is the prior mean, rather than an observation. As expected, the predictions conditional on mean estimates of fecundity (right) have narrow predictive intervals: they include only a subset of the uncertainty, i.e., that contributed by the seed data model assuming known fecundity. Predictions that incorporate the uncertainty in the state–space model itself (left) have broader predictive intervals and provide a more realistic prediction of uncertainty.

We conducted extensive comparisons between predictive intervals for latent states at the population level, with the estimates for latent states available for each individual tree year. These comparisons help identify inconsistencies in the model; the predictive intervals obtained by methods discussed above should agree with the distributions not only of data (e.g., Fig. 14), but also of latent states being estimated in the model. To illustrate, Fig. 15 includes predictive intervals for growth, fecundity, and mortality risk of *Quercus* where the latent states are represented in light green and predictive intervals are in black (a dark understory with $\lambda = 0.1$), red (an intermediate exposure level of $\lambda = 40$), and, for fecundity, dark green (intermediate exposure, conditional on being mature). The sources of uncertainty are parameter uncertainty, random individual effects, year-to-year variation, and process error. In general we find agreement between estimates of latent states and the predicted variation from the model. The latent states for fecund individuals are covered by the predictive distributions conditional on being mature (Fig. 15b; the large number of dots along the bottom of the plot indicates immature individuals). The black and red unconditional fecundity predictions marginalize over the probability of being mature.

RESULTS

Summary of parameter estimates and species responses

Because light is a key resource for which species compete, we discuss this parameter in relation to overall variance in growth and fecundity response. The matrix of fixed effects $\mathbf{A}$ (Eq. 2) contains parameters describing the proportionate responses of diameter growth (A_{41}) and fecundity (A_{42}) to exposed canopy area λ. Species showing large values have a large proportionate response. Thus, species in the genera *Betula*, *Quercus* (*Q. velutina*, *Q. prinus*), *Pinus* (*P. strobus*, *P. rigida*),

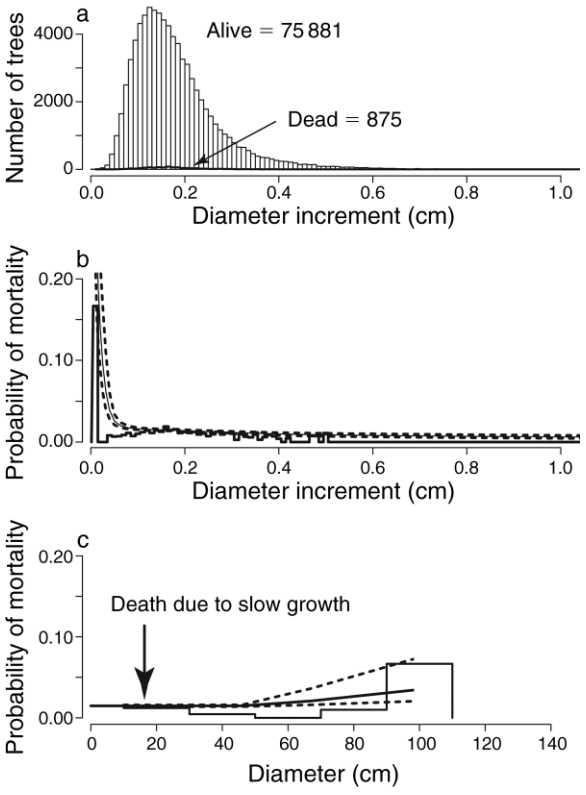

FIG. 11. (a) Mortality data, plotted against growth rate, (b) relative frequency of deaths (histogram) and posterior median and 95% CI for μ_d taken at the mean diameter, and (c) relative frequency of deaths (histogram) and posterior median and 95% CI for μ_D taken at the mean diameter increment. The relationships between growth rate and diameter and survival are given in Eq. 9.

Tilia, and *Fraxinus* have a large proportionate increase in growth with increasing light levels, whereas species in the genera *Acer*, *Quercus* (*Q. phellos*, *Q. rubra*), *Fagus*, and *Pinus* (*P. echinata*, *P. virginiana*) have a small proportionate increase (Fig. 16a). Likewise, *Carpinus*, *Cercis*, and *Fraxinus* have a large proportionate increase in fecundity with increasing light, whereas *Liriodendron*, *Quercus prinus*, and *Cornus florida* have a small proportionate increase with increasing light (Fig. 16b). It is important to bear in mind that these are proportionate, not absolute, responses.

Posterior distributions show species responses to diameter, displayed in Fig. 17 as posterior means by year for 200 *Fraxinus* trees selected at random in different regions (Piedmont = green, Appalachians = red) and light levels (proportional to line thickness). The effects of light are more easily seen from the predictive distributions (Fig. 15), but the trends for individuals over time provide a sense of variation within and among individuals. Individuals in shade grow more slowly, are less likely to be mature, and produce less seed.

When compared among species, mortality risk as a function of growth rate shows a range of patterns (Fig. 18a). Some species had consistently low (*Acer*, *Carya*) or high (*Robinia*, *Cercis*) mortality rates at the for all growth rates. *Liquidambar* had among the highest mortality rates at slow growth and among the lowest mortality rates at high growth. *Cornus* had high mortality rates at all growth rates, most likely due to the spread of Anthracnose (Wyckoff and Clark 2000). The differences among species are evident from Fig. 18b, which shows the mortality rate for individuals growing at 0.1 cm/yr, an intermediate growth rate for most species.

Among species, maturation probability increases with size at different rates for different species (Fig. 18c, e) and with different sensitivities to light (Fig. 18d). Maturation occurs at the smallest diameters for understory species *Cercis, Carpinus,* and *Cornus* and at largest sizes for *Robinia*, *Quercus*, *Carya*, and *Pinus*. It is important to recognize that relationships are shown for the mean ECA for the species in this study, which depends on the distribution of data. In Fig. 18e, we show the degree of increase in maturation diameter from intermediate (ECA = 20) to low light (ECA = 1). The largest differences are for *Pinus*, *Liquidambar*, and *Fraxinus*.

Demographic rates

Most of the variables in the state vector $\mathbf{S}_{ij,t}$ are modeled as latent states, because they are not directly observed or they are not observed every tree-year. The conditional relationships for a latent state m have the following general form:

$$p(\mathbf{S}_{ij,t}[m]) \propto p(\mathbf{S}^{(o)}_{ij,t}[m] \,|\, \mathbf{S}_{ij,t}[m], \boldsymbol{\pi}_o) p(\mathbf{S}_{ij,t}[m] \,|\, \text{process model}, \boldsymbol{\pi}) \quad (10)$$

where $\boldsymbol{\pi}$ and $\boldsymbol{\pi}_o$ are parameters for the process and observations, and $\mathbf{S}^{(o)}_{ij,t}$ is the set of observations. The posterior distribution for each state variable represents a balance of information coming from observations and the process model. For diameter D, the data models include diameter measurements and increment cores. For the state fecundity f, the data model describes transport of seeds from trees to seed traps. The second factor in Eq. 5, the "process" for these two variables, is Eq. 3. Together, the two factors on the right hand side allow uncertainty associated with data and process, making full use of prior information, including previous studies and theory.

Summaries of latent state estimates can be complementary to those for parameter estimates and represent an important component of our analysis. Parameters describe relationships that apply to the species, including overall responses to covariates, between years, and variances. As is clear from Eq. 5, estimates of latent states apply to an individual and year. Estimates for how individuals depart from the overall response is used to test hypotheses, based on summaries within individuals over time, among individuals of a species, and among

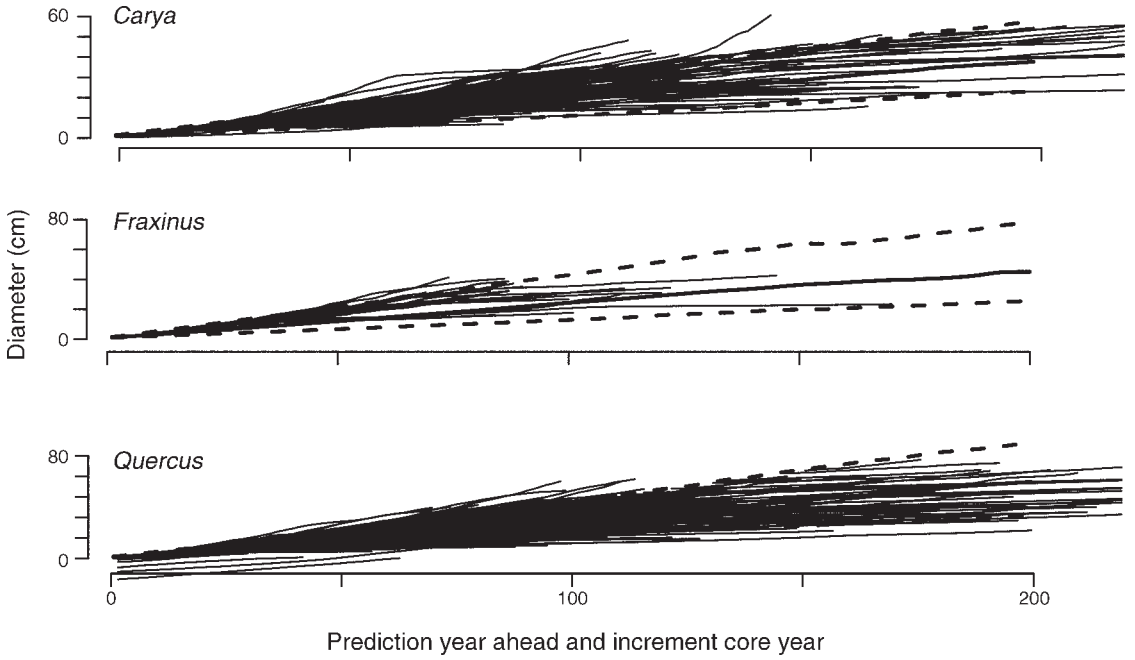

FIG. 12. Comparison of increment data from tree ring data not used in fitting the model (solid lines) and 95% predictive distributions of tree diameter from the model (dashed lines). For predictions, year effects and exposed canopies areas were drawn at random from estimated values.

individuals of different species (Table 1). For each individual there is an estimate of the vector of latent states for diameter growth $\mathbf{d}_{ij}$, fecundity $\mathbf{f}_{ij}$, and survival probability ζ_{ij}. Each vector has length $n_{ij} = T_{ij} - t_{ij}$, i.e., from the time of first observation until death or censoring. There is a credible interval for each latent state for each tree-year. Primarily based on estimates of latent states we synthesize evidence for trade-offs within populations and among species, and apply them to the three hypotheses.

Among individuals (within populations).—We posed the alternative hypotheses that populations show negative or positive correlations among individuals between demographic rates, calculated for individual means ($\overline{d_{ij}}$, $\overline{f_{ij}}$) (Table 2). Negative correlations are expected if there are trade-offs in allocation (Fig. 1b). Positive correlations are expected if populations are dominated by healthy vs. unhealthy individuals (Fig. 1d). Broad overlap is expected (correlation near zero) if individuals are regulated by large numbers of factors (Fig. 1c).

We found correlations ranging from −0.5 to 0.5 and large differences between species within the same genus. Fig. 19 shows examples of both extremes. For *A. pennsylvanicum* and *Nyssa sylvatica* individuals with rapid growth have low fecundity, and vice versa, as consistent with the trade-off hypothesis. Species with positive correlation are consistent with the alternative hypothesis. This correlation could depend on other covariates. We examined whether negative correlations were related to variation in fecundity, which is highest for shade-tolerant species that tend to be reproductive in both sun and shade, and several species in the genus *Pinus*, as shown by the vertical axis in Fig. 19. We did not find a tendency for negative correlation between

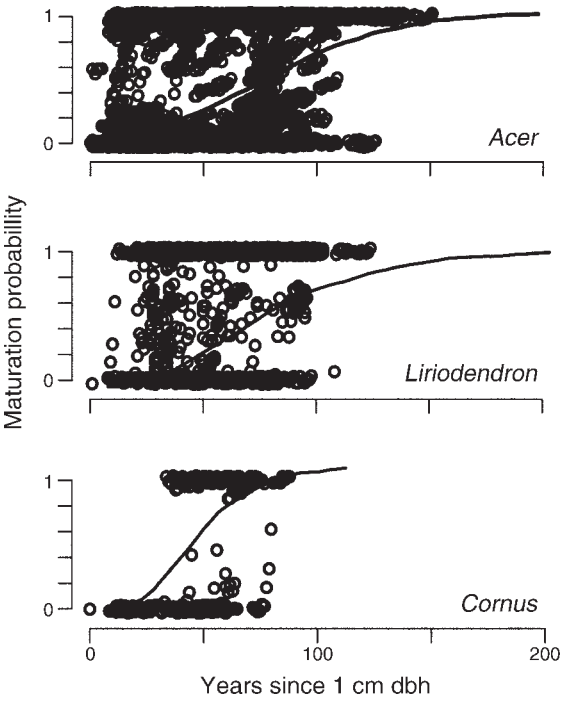

FIG. 13. Maturation age predictive means (smooth curves) compared with individual estimates of trees aged by increment cores (dots) for three species.

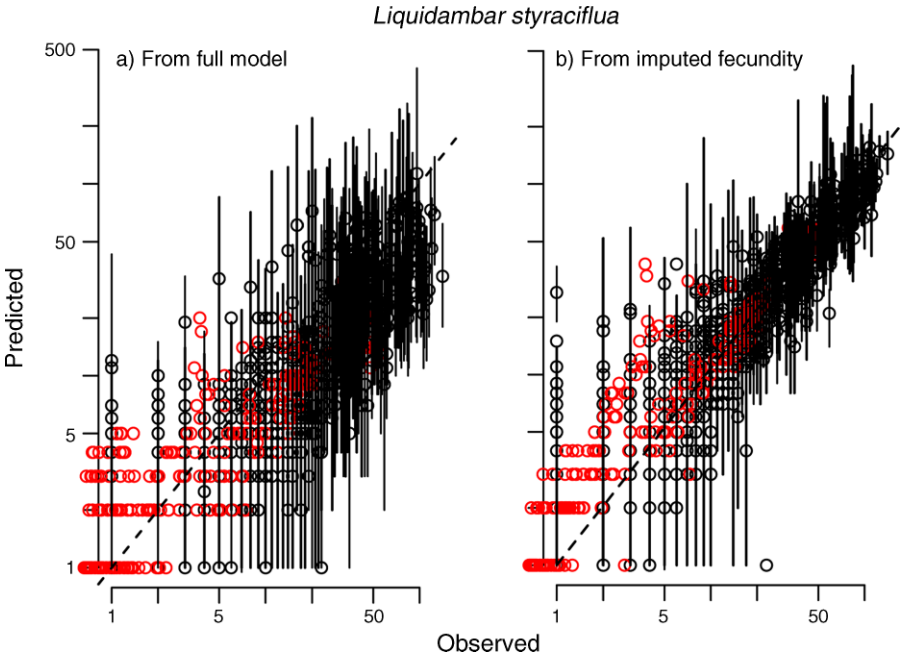

FIG. 14. Predictions for seed data from *Liquidambar styraciflua* conditioned (a) on mean estimates of covariates and (b) on posterior mean estimates of fecundity on a log scale, so zeros are not shown. Predictive intervals are broader in panel (a) because they integrate not only uncertainty associated with dispersal and sampling, but also in the state space model of fecundity. Red circles are prior values on the horizontal axis.

growth and fecundity to be related to variation in fecundity. Many of the species with high variation among individuals are dioecious, and males are not included in the analysis (*Nyssa*, *Acer rubrum*, *Fraxinus americana*).

In summary, among individuals, we find species showing patterns expected if there are trade-offs among individuals (negative correlation) and if individuals differ primarily in overall health (positive correlation). However, most species are dominated by low correlation among individuals, showing that neither hypothesis dominates and suggests that individuals respond to a large number of factors.

Among species.—There is no evidence for trade-offs among species in the dimensions typically considered in demographic studies (Fig. 20), using calculations based on species differences $(\bar{d}, \bar{f}, \bar{\zeta})$ for individuals subject to different levels of canopy exposure λ. In addition to these demographic rates, we evaluated "colonization potential," estimated as the number of seeds dispersed >50 m from the parent:

$$\int \left[\int_{50}^{\infty} \oint_{2\pi} f_{ij,t} K_{\omega}(r \mid u) p(f_{ij,t}, u)\, d\omega\, dr \right] d(f_{ij,t}, u) = \int \frac{f_{ij,t}}{1 + 50^2/u} p(f_{ij,t}, u)\, d(f_{ij,t}, u)$$

where $p(f_{ij,t}, u)$ is the posterior density for fecundity and the dispersal parameter u (Eq. 3).

Even among mean values for species, we do not observe negative correlations between high-light growth and low-light survival, low-light growth and high-light fecundity, high-light fecundity and low-light survival (left panels of Fig. 20), or colonization at 50 m and low-light mortality. The correlations among species mean values are all weak, but positive, not negative. Moreover, the variation among individuals in these rates overwhelms differences among species (right panels of Fig. 20). The bars on the right side of Fig. 20 are not error bars, but rather indicate 95% of the mean values for individuals of each species (Table 1). Broad overlap is inconsistent with the limiting similarity that would be required if coexistence depended on partitioning of a few niche axes (Fig. 1).

To determine the extent to which fecundity, growth, and mortality risk change in combination with light availability, we examined response vectors, averaged by species (Fig. 21). Because these are log values they are proportionate responses. The difference between demographic rates at low and high light provides evidence of plasticity to respond to high resource conditions. For mature trees, the species with the largest differences between low and high light for fecundity are *Ulmus americana* and *Tsuga* (Fig. 21a), those with the largest differences for growth are *Betula lenta* and *Tsuga canadensis* (Fig. 21a), and those with the largest differences for mortality risk are *Fagus* and *Liriodendron* (Fig. 21b, c). For *Fagus*, the magnitude of change in mortality risk results from the fact that it is still able to

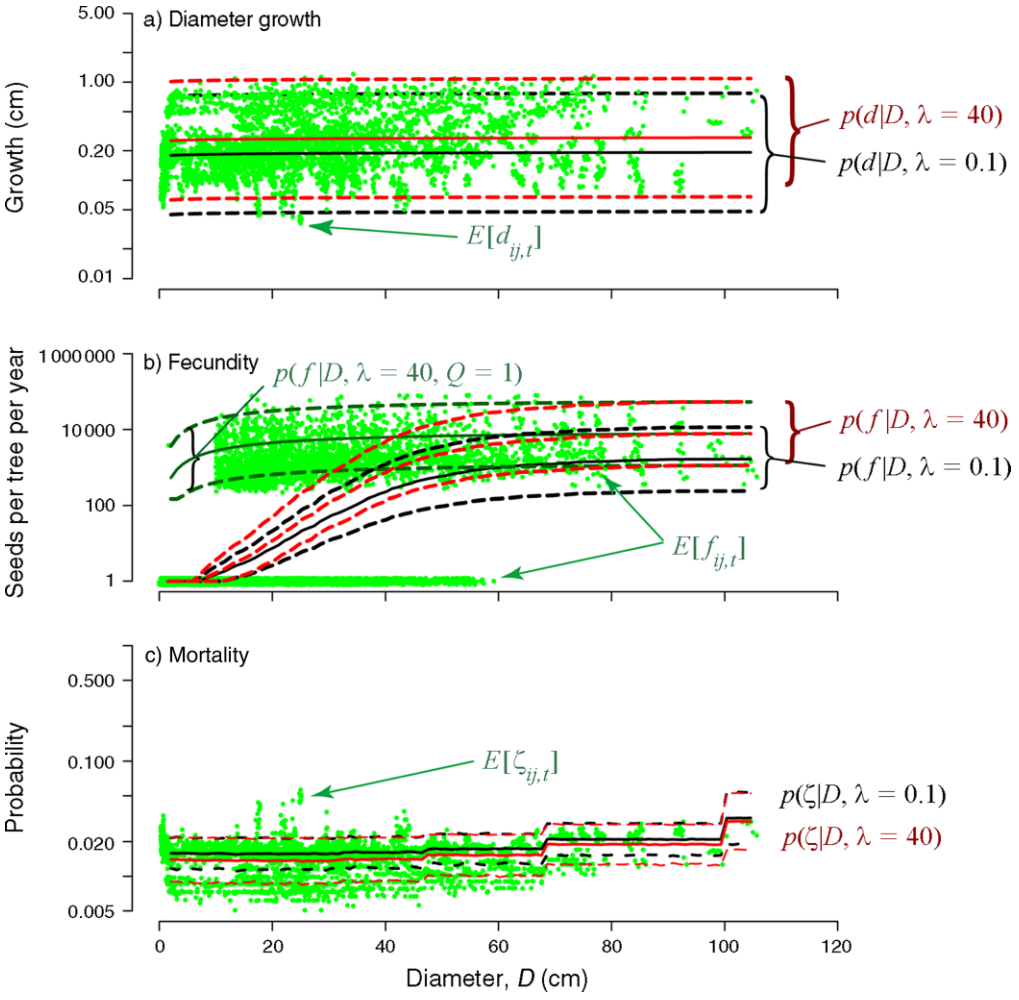

FIG. 15. Posterior mean estimates of latent states (green dots) and predictive intervals for low (black lines) and high (red lines) canopy exposure λ. Included in panel (b) is a second set of predictive intervals for fecundity conditioned on mature status and high canopy exposure (dark green line). Zero values (immature status) are jittered and plotted as 1's to make them visible on this log scale.

survive at extremely low growth rates (Fig. 22b, c). For immature trees, species showing large proportionate growth responses to light include *Betula lenta*, *B. alleghaniensis*, *Tsuga*, *Pinus rigida*, and *Acer barbatum*.

Overall demographic response is summarized in Fig. 21d by the Euclidean distance in these three dimensions, where they are shown for immature trees (black) and mature trees (red). For immature trees, the largest proportionate responses were for shade-tolerant species, including species in the genera *Acer*, *Betula*, and *Tsuga*, but also *Pinus rigida*. For large trees, rankings changed due to the fact that some species showed large fecundity responses to light availability (*Ulmus* and *Pinus*).

In summary, we find differences among species, but not those that could explain coexistence by low dimensional trade-offs. Species each show different combinations of life history interactions, even when viewed in the low-dimensional space accommodated by this analysis. However, results do not show that species differ in the specific ways (e.g., trade-offs) and to the degree (e.g., limiting similarity) that would promote coexistence (Fig. 1a). We do find the large variation within individuals and populations consistent with high-dimensional regulation of diversity (compare Figs. 1c and 20), but summaries presented thus far do not demonstrate that such regulation is occurring. If variation is structured in a way that contributes to coexistence then correlations among individuals of different species should be less positive than are those of the same species (Fig. 1e). The relevant correlations are $c_d(i, i')$ from Table 2, where comparisons are done for individuals i and i' of the same and of different species that occur on the same plot j. Here the evidence is strong.

In Figs. 22 and 23, we evaluated correlations between demographic rates for every pair of individuals that occur on the same plot (Table 2) and compiled them in histograms for all species pairs. These are correlations

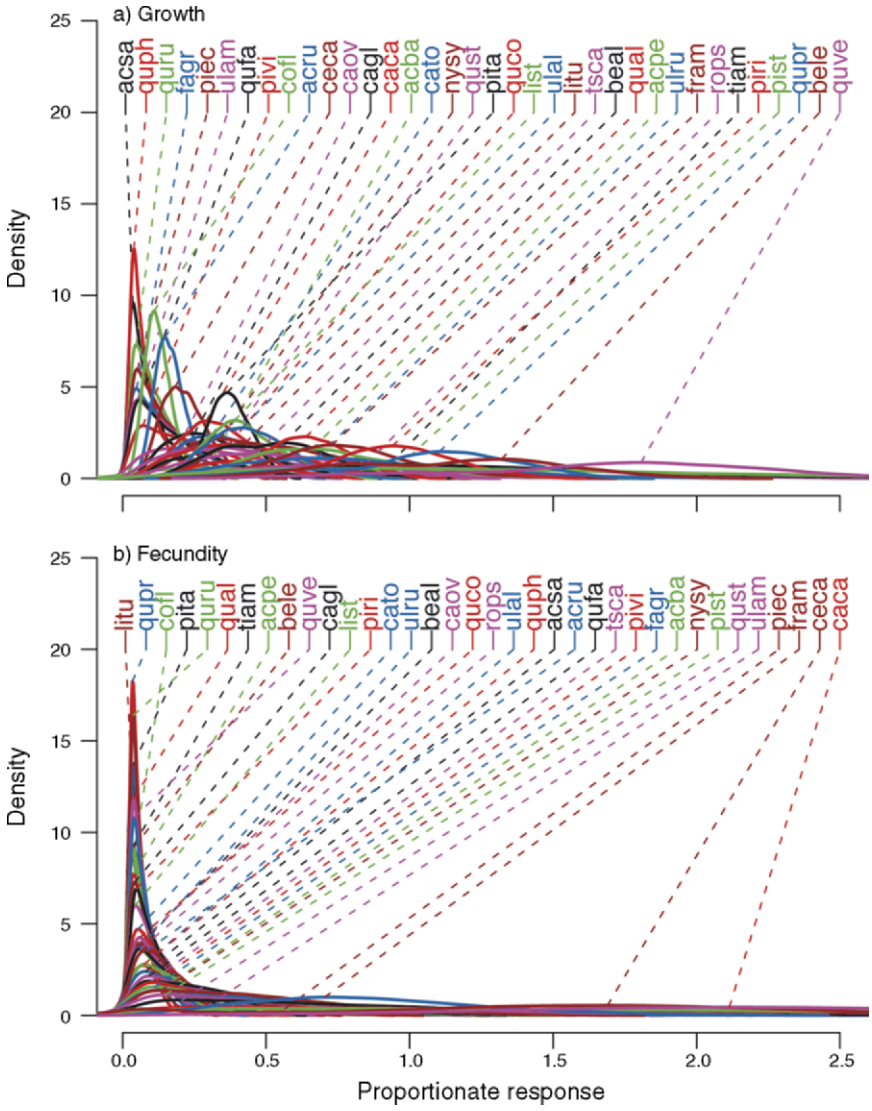

FIG. 16. Species comparisons of posterior densities for light response parameters: (a) growth; (b) fecundity. Species with the highest values have the largest proportionate response to canopy exposure, and vice versa. See Table 4 for key to species abbreviations.

in response between each pair of individuals over years (Fig. 1e). The lower left panels (blue) are for growth rates, and the upper right (black) for fecundity. These correlations were overwhelmingly lower when comparing individuals of different species (off-diagonal panels of Fig. 22) than when comparing individuals of the same species (diagonal panels of Fig. 23). Black boxes indicate the highest average fecundity correlation in a row, and blue boxes indicate the highest average growth correlation in a column. For both growth and fecundity, the correlations between individuals of the same species that are growing in the same stand are overwhelmingly higher, on average, than between individuals of different species. This result is reasonable, given that they most closely share physiology and allocation characteristics.

DISCUSSION

Results establish that traditional trade-offs do not explain the diversity of these forests, but high-dimensional differences, which are evident at the individual level, show the structure that is required if it is responsible for coexistence. We found differences among species in every dimension we examined, but there is also broad overlap (Figs. 16, 18, 21). These species-level differences are not consistent with trade-off assumptions (Fig. 1a), showing not only lack of limiting similarity, but also lack of the trade-offs in species means (Fig. 20). The large variation among individuals is structured in a way that can promote coexistence through high-dimensional regulation. The comparisons of responses between individuals of the same and different species are

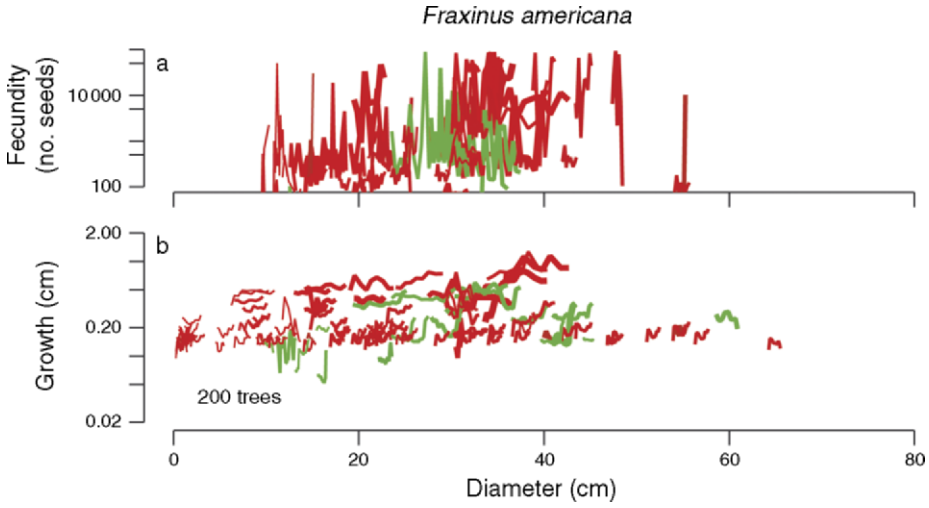

FIG. 17. Predictive mean demographic rates for 200 *Fraxinus americana* trees selected at random. Line thickness is scaled to canopy exposure. Line colors are red for highest elevation and green for lowest elevation. Note the log scales.

consistent with the hypothesis that species partition environmental variation. Individuals respond more like others of the same species in terms of both growth and fecundity. Because growth determines size, and thus light capture, and fecundity determines competition for recruitment sites, these tendencies to compete more with individuals of the same species can accumulate over time, providing a mechanism to promote and maintain diversity.

Trade-offs among species

If diversity maintenance results from partitioning one or a few niche axes, there must be not only strict parameter trade-offs, but also limiting similarity: trait syndromes cannot be arbitrarily similar (MacArthur and Levins 1964, Pacala and Tilman 1994; Fig. 1a). Simple trade-offs do not emerge from our analysis, which included high-light growth vs. low-light survival, low-light growth vs. high-light fecundity, high-light fecundity vs. low-light mortality, and colonization vs. low light mortality. The correlations are near zero and have the wrong sign (Fig. 20). By estimating observation errors and variation within individuals and over time, we show that variation among individuals of the same species exceeds the variation of means among species (Fig. 20, right-hand panels).

Instead of trade-offs in a few dimensions, species partition environmental variation in ways that promote coexistence in a manner consistent with many dimensions of variation (Figs. 22 and 23). Individual differences result when a large number of factors contribute to diversity. Individual-scale inference shows that interspecific correlations are lower than intraspecific correlations, the principle requirement if species compete more with their own species, and thus partition environmental variation (Figs. 22 and 23). This result does not challenge the view that low-dimensional trade-offs can contribute to coexistence, only that they explain diverse communities. Traditional trade-offs, including those involving spatiotemporal variation, explain coexistence of a few competitors, not dozens to hundreds. The species differences occur in many dimensions, most of which cannot be directly observed in a single study. The demonstration that those differences contribute to coexistence requires individual-level data (replication at the individual level, over time) and inference. If many factors control diversity, species differences remain a requirement, but there is no reason to expect them in a few dimensions.

The observation of strong individual variation is consistent with previous observations for reproduction (Sharp and Sprague 1967, McCarthy and Quinn 1992, Clark et al. 2004, Mitton and Duran 2004, LaDeau and Clark 2006), growth (Clark et al. 2007*b*, Mohan et al. 2007), and mortality (Vaupel et al. 1979, Carey et al. 1992). Part of the variation among individuals can be ascribed to covariates that can be measured or inferred using models. The most readily observed examples include site variation in light availability and soil moisture. Additional variation may be captured with random individual effects (Vaupel et al. 1979, Clark et al. 2003, 2004, Ibáñez et al. 2008). The random effects covariance matrix (Eq. 3b) summarizes this variation among individuals that remains after accounting for covariates. Random individual and temporal effects (RITEs) exceed the variation explained by covariates; the individual differences are the basis for the spread in panels on the right-hand side of Fig. 20. Whereas average demographic rates do not yield much insight concerning mechanisms of coexistence, large variation among individuals indicates that the species can be doing well in some locations and poorly in others. This is the expectation if niche differences are high dimensional. If they contribute to coexistence, we expect

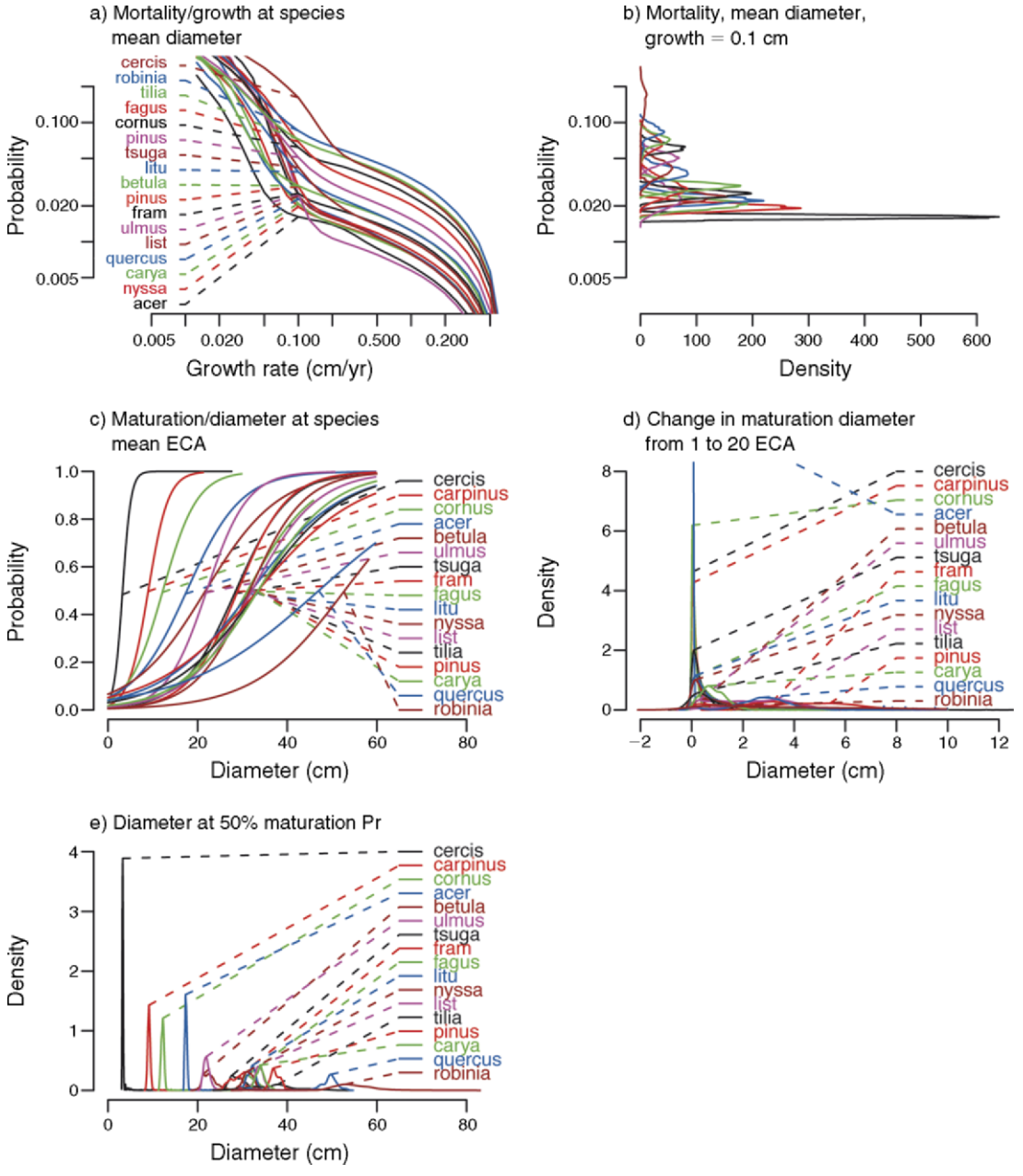

FIG. 18. (a) Posterior mean mortality risk plotted against diameter growth rate. (b) Posterior density for mortality risk at a growth rate of 0.1 cm. (c) Posterior mean probability of maturation at different diameters. (d) Predictive density for increased light exposure on mean maturation diameter. (e) Posterior density for diameter at a maturation probability of 0.5.

intraspecific correlations to exceed interspecific correlations (Figs. 22 and 23).

The lack of evidence for low-dimensional trade-offs in our study could be misinterpreted in several ways. First, it is not inconsistent with studies that find correlations between traits for small numbers of species. A trade-off between high-light growth and low-light survival has been observed for particular pairs of species (e.g., Kitajima 1994, Walters and Reich 1996, Dalling and Hubbell 2002). We could extract examples of species from our analysis showing such differences (e.g., *Liquidambar* grows faster than *Tsuga* in high light, but suffers higher mortality risk in low light). The lack of correlation in Fig. 20 does not deny such relationships between selected pairs of species. Rather, it shows that these trade-offs are not sufficiently general to explain coexistence of large numbers of species.

While not inconsistent with correlations reported for selected pairs of species, our results are inconsistent with studies that find community-wide correlations. Welden

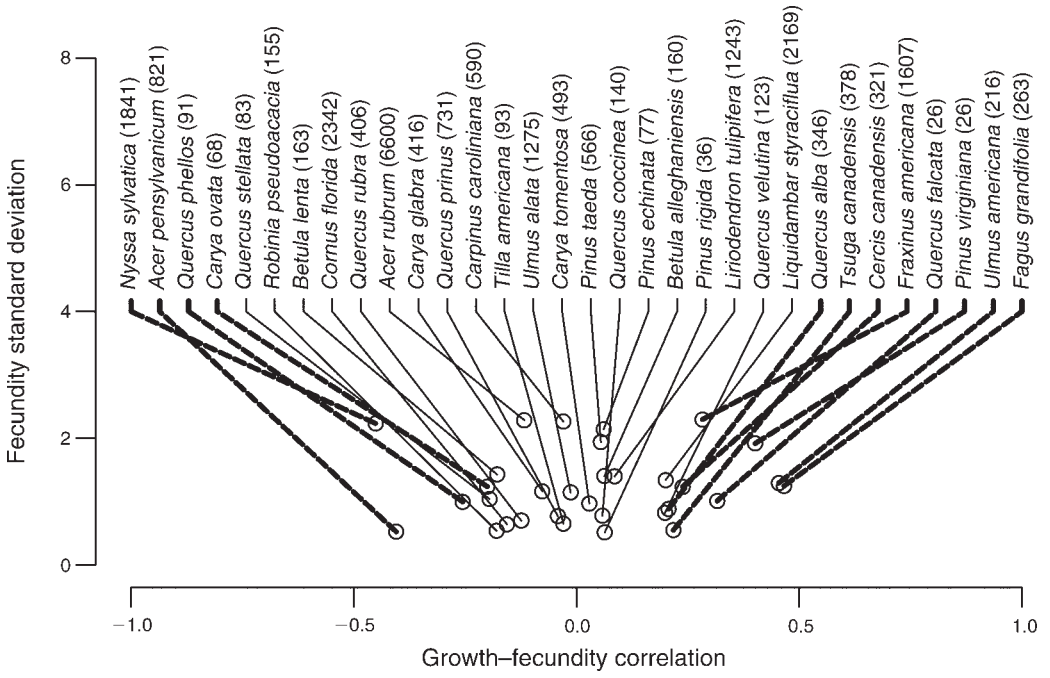

FIG. 19. Correlations within populations (among individuals) in growth and fecundity plotted against the standard deviation in fecundity, including only mature and (for dioecious species) individuals with posterior probability of being female >0. Thick dashed lines show species having correlation <−0.2, and >0.2. Numbers of mature individuals that contributed to estimates are indicated in parentheses.

et al. (1991, see also Wright 2002) and Gilbert et al. (2006) find such correlations from tropical forests in analyses containing as many or more species than included here. Although many of the same species in our study are also included in the analysis of Pacala et al. (1996), and we present essentially the same trade-off axes in Fig. 20, we do not find correlations. Differences in demographic rates between sites could be substantial: we should not expect to observe the same relationships in the Southeast as did Pacala et al. (1996) in the Northeast. The current analysis does not include seedlings (only trees >2 m in height are included), so some of the correlations reported by studies such as Gilbert et al. (2006) could emerge when analysis of seedlings is included (D. Bell, M. Hersh, I. Ibanes, and J. S. Clark, *unpublished manuscript*). An additional difference between these studies is the analysis. Moreover, these results are not the first to show lack of trade-offs in low-light survival and high-light growth (Clark and Clark 1992, Sipe and Bazzaz 1995).

A second potential misinterpretation of our results concerns broad overlap among species (i.e., lack of significant differences) in trait or demographic space (Fig. 20), which can be taken as evidence of species sameness. Neutral theory proposes that species do not differ or that identical demographic rates and fitness makes species differences unimportant. Empirical evidence for this view comes from estimates of species-level demographic rates. The detailed demographic inference possible in this study reveals large differences among species in every respect, all of which affect fitness, including maturation schedules (Fig. 18), sex ratios (not shown), growth, and fecundity (Figs. 10, 16, 21), dependence on covariates (Figs. 16 and 18e), survival (Fig. 18), and responses over time (Fig. 10). Moreover, treatment of species identity as a random effect (Condit et al. 2006) necessarily makes species appear more similar than they actually are.

If we find that species differ in all of their demographic schedules, and these schedules, by definition, determine population growth and fitness, how is it possible that traditional inference can lead to the conclusion that demographic rates and fitness values do not importantly differ among species? Consider how confusion can arise using the example case of coexistence, simply for purposes of discussion. Neutral theory proposes that species having the same average fitness coexist by neutral drift. However, species that coexist by partitioning the environment always have the same average fitness, with $r = 1/N\ dN/dt = 0$ and $R_0 = 1$. The fact that $r = 0$ for all species simply means that abundances are not changing; it provides no insight concerning niche partitioning (Clark 2009). Species can have the same average fitness, but at different abundances and with individuals that are responding in many ways. Differences in abundance are one of the critical manifestations of species differences. Whereas the average fitness values for coexisting species are the same, the variation in fitness that is crucial for coexistence is organized as differences among individu-

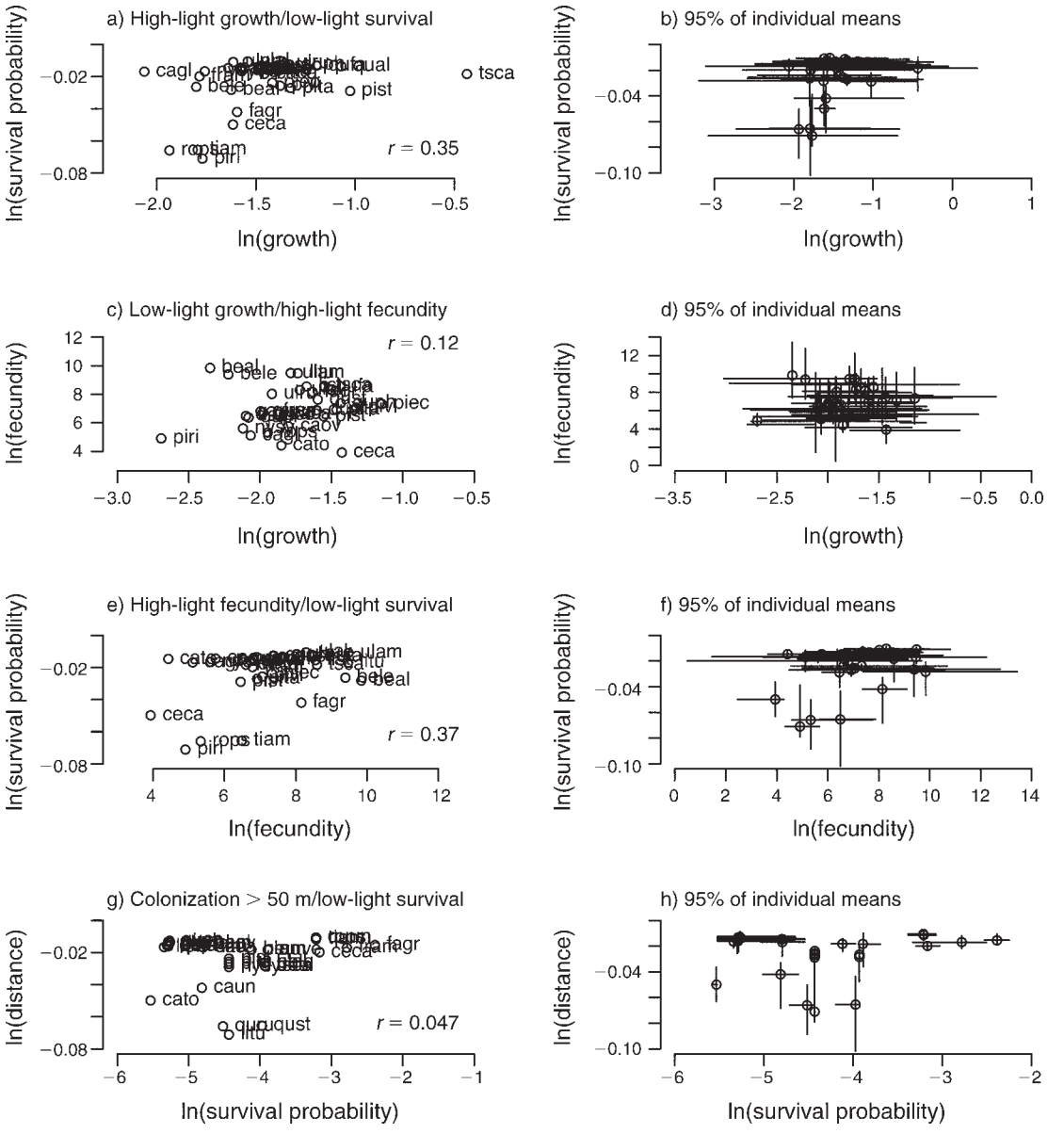

FIG. 20. Relationship among species in terms of (a, b) capacity to grow fast at high light vs. survival in low light, (c, d) growth in low light vs. fecundity in high light, (e, f) fecundity in high light vs. survival in low light, and (g, h) colonization at long distances vs. survival in low light. At left (a, c, e, g) are plotted means taken over all individuals of a species, $(\overline{d}, \overline{f}, \overline{\zeta})$. At right (b, d, f, h), intervals span 95% of individual means $(\overline{d_{ij}}, \overline{f_{ij}}, \overline{\zeta_{ij}})$ for a species and include only variation among individuals; they exclude observation error and parameter uncertainty.

als. Averaged over a species, demographic rates can appear similar simply because each species is most abundant in locations where individuals have survived to be observed. Without knowing how demographic rates vary across the sites where individuals are found and the high-dimensional variation that occurs there, the average demographic rates do not provide much insight about coexistence.

Recognition that high dimensionality could be important for diversity is not new (Hutchinson 1961, Levin 1998). Many hypotheses proposed and tested in recent years bring additional dimensions to traditional mechanisms. Tilman (1982, 1988) included explicit resources. Competition can vary with life history stage (Grubb 1977, Denslow 1987), and species may possess traits (Tilman 1994, Bonsall et al. 2004), experience losses to natural enemies or disturbance (Clark 1992, Pacala and Crawley 1992), and/or forage in ways (MacArthur 1958, Tilman 1988, Kohyama 1993, Huston and DeAngelis 1994) that effectively promote diversity. Predation and competition can operate together (Chase et al. 2002, Amarasekare 2007). The Janzen Connell effect could

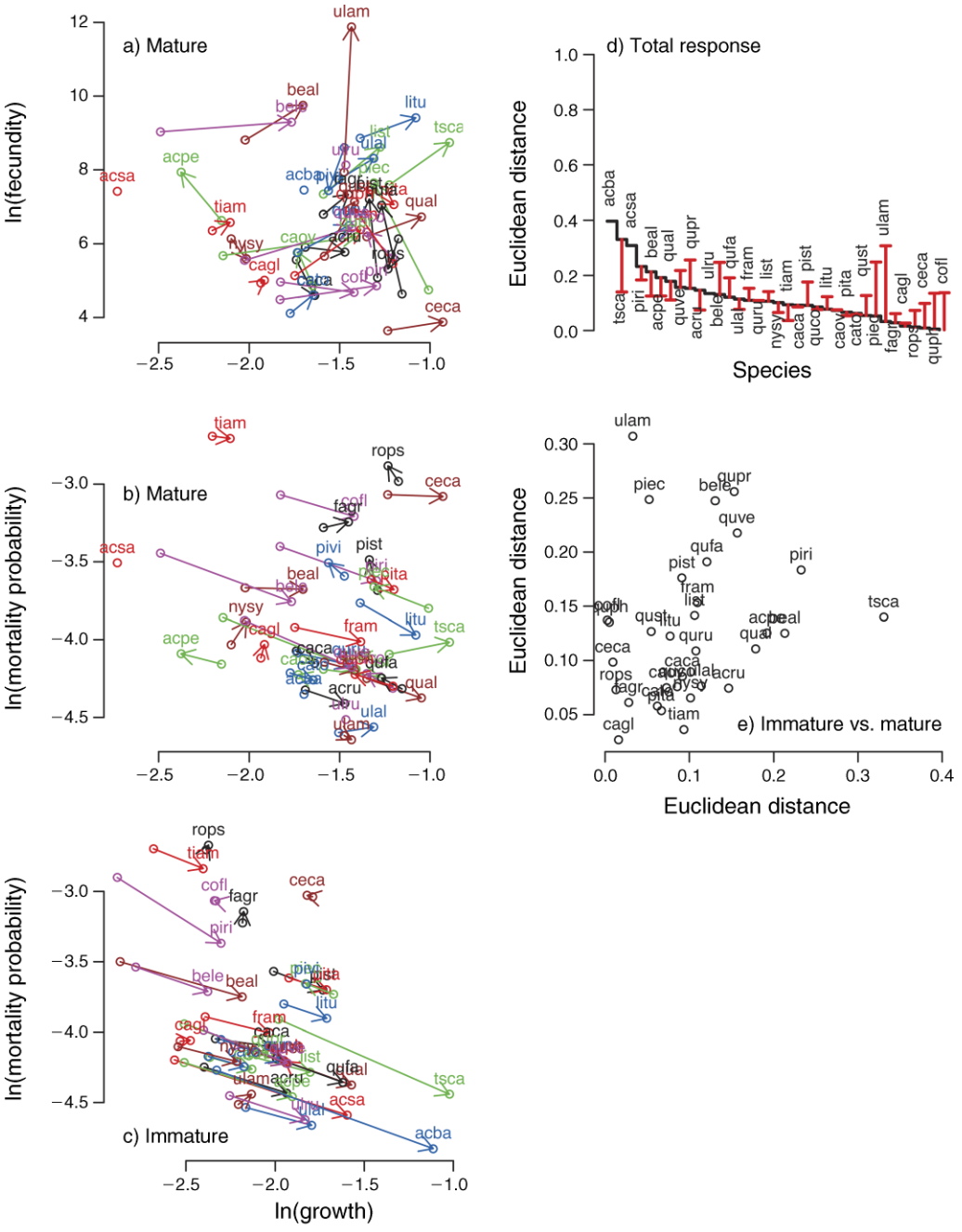

FIG. 21. Light-response vectors by species for two size classes (mature and immature). Vectors point from demographic rates at low light (suppressed in understory) to those for high light (exposed canopy area = 40 m^2). Plots (a)–(c) show comparisons with growth rate on the horizontal axis. Panel (d) shows the total response (Euclidean distance) for immature (black) and mature (red) trees. Panel (e) is the comparison of responses for immature and mature trees. See Table 4 for key to species abbreviations.

result not only from host-specific natural enemies, but also from host-specific combinations (Clark and Hersh 2009). These studies represent specific ways in which interactions increase dimensionality.

Even a relatively small number of "factors" can potentially provide many dimensions along which species can differ. Temporal variability, either intrinsic (Huisman and Weissing 1999) or extrinsic (Levins 1979, Armstrong and McGehee 1980), can effectively increase dimensionality, resulting in different and shifting combinations of limitations. Spatial variation in just a few resources could contribute to coexistence of a number of species (Tilman 1982). Physiological trade-offs that could contribute to niche partitioning

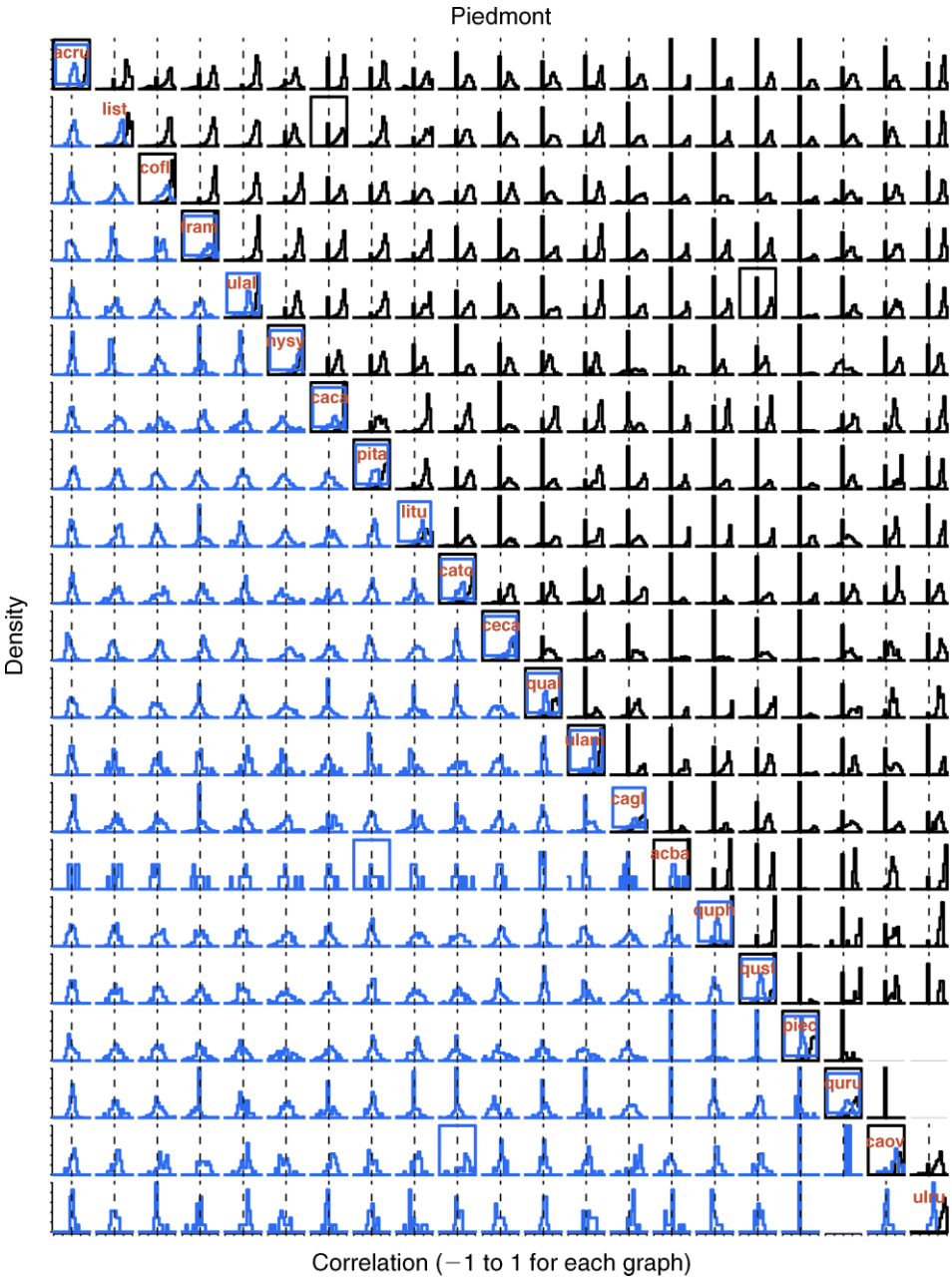

FIG. 22. Histograms of correlations among individuals of the same (diagonal) and different (off-diagonal) species growing together on the same plot for all species in the southern Appalachian sites. The lower left shows growth rate (blue); upper right is fecundity (black). Each histogram is the comparison for species listed on the diagonal. See Table 4 for key to species abbreviations. Missing panels are comparisons for which either of the pair has <20 individuals at all sites. The vertical dashed line indicates zero correlation. Framed plots have the highest average correlation for growth (blue) or fecundity (black). Species are presented in order of abundance, from highest (acru) to lowest (ulru).

in many dimensions include carbon allocation constraints to growth, storage, and reproduction (Reznik 1985, Obeso 2002, Würth et al. 2005, Myers and Kitajima 2007), interrelated constraints on leaf thickness, longevity and nitrogen content (Wright et al. 2004), and wood architecture needed to balance strength, hydraulic efficiency, and other attributes (Chave et al. 2009).

The clear differences between correlations between and within species (Figs. 22 and 23) indicate that partitioning is occurring, but not along any one or a few of the dimensions traditionally invoked to explain

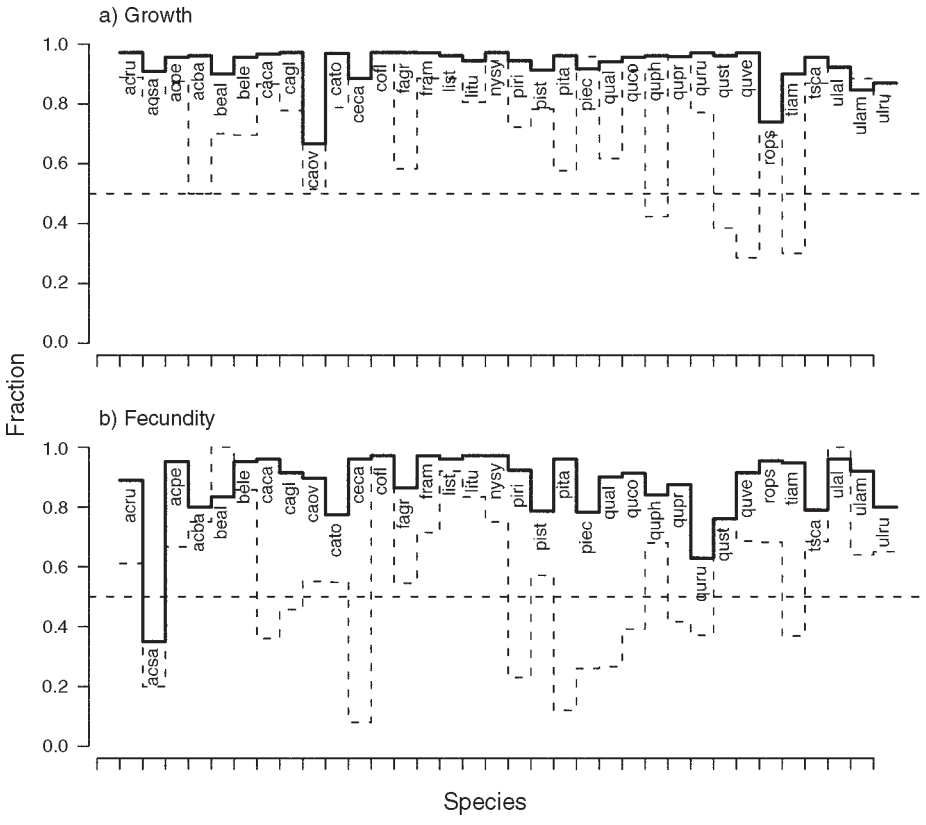

FIG. 23. The fraction of correlations between individuals of two species for which the correlation between individuals of the same species is greater than those for individuals of different species.

diversity (Fig. 20). The species partitioning requires individual scale data and inference.

Trade-offs within populations

The alternative hypotheses concerning trade-offs within species (Fig. 1b–d) make predictions that our modeling approach can evaluate, because we can estimate latent states associated with individuals. On the one hand, populations may consist of coexisting phenotypes, with different individuals specializing in different activities. In this case we expect negative correlation among individuals in terms of their allocation to different activities. We observe this negative correlation for some species, those to the left of Fig. 19. Alternatively, individuals can vary in overall health status that affects multiple demographic rates. We observe positive correlations for species to the right of Fig. 19. If populations are dominated by differences between healthy and unhealthy individuals, then trade-offs might be most important for the least healthy individuals. For example, at high resource levels (e.g., high light) there could be both rapid growth and high fecundity. By contrast, resource deprivation might demand a trade-off: grow now and reproduce later. The vertical axis in Fig. 19 does not show that species characterized by negative correlation tend to also have high variability in fecundity. The possibility that these correlations could depend on individual health could be explored in subsequent studies involving detailed measurements on individuals of different species. However, for most species the correlations are low, falling on the interval (–0.3, 0.3), which is consistent with a large number of regulating factors.

The finding that populations consist of individuals with a large range of health statuses (Fig. 19) provides a link to the species level result, which indicates the importance of individual subjected to variation in many dimensions (Figs. 22 and 23). This mixture of health statuses reflects heterogeneity in controls that would be needed if species differences at the individual level contribute to coexistence.

CONCLUSIONS

The emphasis of biodiversity science on simple explanations is critical for identifying generalities that might explain pervasive patterns. It is responsible for a deep understanding of how trade-offs in response to a few factors can contribute to biodiversity and patterns like succession. Recognition of the importance of life history and resources owes much to the analysis of simple models that isolate their impacts and to empirical study of their potential importance in nature. At the

same time, the goal of a simple explanation for the coexistence of large numbers of competing species can become counterproductive, when failure to identify the trade-offs required to justify a low-dimensional view of nature leads to nonspecific explanations such as "stochasticity" or "equalizing forces" or simply failing to adopt a realistic approach to current and future preservation of species. As important as simplicity is, many disciplines have embraced the need to study processes that lack a low-dimensional interpretation (O'Hagan and West 2009). Biodiversity is as complex as the problems that have motivated other disciplines to look toward models that accommodate more interactions, human health being one obvious example. Simple models have had an important role in ecology, but additional progress on hard problems like biodiversity now requires a more realistic approach. The hierarchical approach applied here holds promise, identifying that species do partition the environment in ways that can promote diversity, but only if there are many ways in which species differ. Productive study requires individual scale inference.

If large models are to provide guidance they need to accommodate complexity in the simplest possible ways. The insight concerning species differences here owes much to the attention to how variation might be structured and what that structure might reveal about species interactions. Although the model is large, it actually represents the antithesis of complexity, limiting inference to a small number of relationships known to have critical importance and using stochastic terms to stand in for the relationships that cannot be observed. Our results do not recommend an effort to 'measure everything,' but instead focus on ways to move forward with limited knowledge. Finding that variation among individuals is structured in ways that would be required to promote diversity indicates the importance of moving beyond simple mechanisms.

Acknowledgments

Field, lab, and remote sensing involved a large number of undergraduates and research technicians, including Nathan Buchanan, Melissa Burt, Alyssa Cooper, Natalia Dorfman, Maryana Draga, Amy Hamilton, Saida Ismayilova, Amber Loucks, Allen McBride, Lauren Nichols, Clint Oakley, Luke Pangle, Danielle Racke, Quentin Read, Sarah Rorick, Greta Schmoyer, Jason Styons, Emily White, Miranda Welsh, Jamie West, John Williamson, and Nathan Welch. We thank Maria Uriarte and three anonymous reviewers for comments on the manuscript. The research was supported by NSF grants BSR-9444146, DEB 9453498, DEB-9632854, DEB-9981392, IDEA-0308498, DEB 0425465, SEII 0430693, and DDDAS 0540347 and by several Dissertation Improvement Grants.

Literature Cited

Abrams, P. A. 1988. How should resources be counted? Theoretical Population Biology 33:226–242.

Amarasekare, P. 2007. Trade-offs, temporal variation, and species coexistence in communities with intraguild predation. Ecology 88:2720–2729.

Armstrong, R. A., and R. McGehee. 1980. Competitive exclusion. American Naturalist 115:151–170.

Assmann, E. 1970. The principles of forest yield study. Pergamon, Oxford, UK.

Baraloto, C., D. E. Goldberg, and D. Bonal. 2005. Performance trade-offs among tropical tree seedlings in contrasting microhabitats. Ecology 86:2461–2472.

Barker, D. J. P. 1998. Mothers, babies, and health in later life. Churchill Livingstone, Philadelphia, Pennsylvania, USA.

Batista, W. B., W. J. Platt, and R. E. Macchiavelli. 1998. Demography of a shade-tolerant tree (*Fagus grandifolia*) in a hurricane-disturbed forest. Ecology 79:38–53.

Beckage, B., and J. S. Clark. 2005. Does predation contribute to tree diversity? Oecologia 143:458–469.

Berliner, L. M. 1996. Hierarchical Bayesian time series models. Pages 15–22 *in* K. M. Hanson and R. N. Silver, editors. Maximum entropy and Bayesian methods. Kluwer Academic, Dordrecht, The Netherlands.

Bonsall, M. B., V. A. A. Jansen, and M. P. Hassell. 2004. Life history trade-offs assemble ecological guilds. Science 306: 111–114.

Bradley, D. J., G. S. Gilbert, and J. B. H. Martiny. 2008. Pathogens promote plant diversity through a compensatory response. Ecology Letters 11:461–469.

Cadotte, M. W., D. V. Mai, S. Jantz, M. D. Collins, M. Keele, and J. A. Drake. 2006. On testing the competition-colonization trade-off in a multispecies assemblage. American Naturalist 168:704–709.

Canham, C. D. 1988. Growth and canopy architecture of shade tolerant trees: response to canopy gaps. Ecology 69:786–795.

Canham, C. D. 1989. Different responses to gaps among shade-tolerant trees species. Ecology 70:548–550.

Carey, J. R., P. Liedo, D. Orozco, and J. W. Vaupel. 1992. Slowing of mortality rates at older ages in large medfly cohorts. Science 258:457–461.

Chapin, F. S., III, L. R. Walker, C. L. Fastie, and L. C. Sharman. 1994. Mechanisms of primary succession following deglaciation at Glacier Bay, Alaska. Ecological Monographs 64:149–175.

Chase, J. M., P. A. Abrams, J. P. Grover, S. Diehl, P. Chesson, R. D. Holt, S. A. Richards, R. M. Nisbet, and T. J. Case. 2002. The interaction between predation and competition: a review and synthesis. Ecology Letters 5:302–315.

Chave, J., D. Coomes, S. Jansen, S. L. Lewis, N. G. Swensen, and A. E. Zanne. 2009. Towards a worldwide wood economics spectrum. Ecology Letters 12:351–366.

Chesson, P. 2000*a*. Mechanisms of maintenance of species diversity. Annual Review of Ecology and Systematics 31: 343–366.

Chesson, P. 2000*b*. General theory of competitive coexistence in spatially varying environments. Theoretical Population Biology 58:211–237.

Chesson, P., and J. J. Kuang. 2008. The interaction between predation and competition. Nature 456:235–238.

Christensen, N. L., and R. K. Peet. 1984. Convergence during secondary forest succession. Journal of Ecology 72:25–36.

Clark, D. A., and D. B. Clark. 1992. Life history diversity of canopy and emergent trees in a Neotropical rain forest. Ecological Monographs 62:315–343.

Clark, J. S. 1992. Density-independent mortality, density compensation, and gap formation in plant populations. Theoretical Population Biology 42:172–198.

Clark, J. S. 2005. Why environmental scientists are becoming Bayesians. Ecology Letters 8:2–14.

Clark, J. S. 2007. Models for ecological data. Princeton University Press, Princeton, New Jersey, USA.

Clark, J. S. 2009. Beyond neutral science. Trends in Ecology and Evolution 24:8–15.

Clark, J. S. 2010. Individuals and the variation needed for high species diversity. Science 327:1129–1132.

Clark, J. S., M. Dietze, P. Agarwal, S. Chakraborty, I. Ibanez, S. LaDeau, and M. Wolosin. 2007*a*. Resolving the biodiversity debate. Ecology Letters 10:647–662.

Clark, J. S., M. Dietze, I. Ibáñez, and J. Mohan. 2003. Coexistence: how to identify trophic trade-offs. Ecology 84: 17–31.

Clark, J. S., and A. E. Gelfand, editors. 2006. Hierarchical modelling for the environmental sciences. Oxford University Press, Oxford, UK.

Clark, J. S., and M. H. Hersh. 2009. Inference when multiple pathogens affect multiple hosts: Bayesian model selection. Bayesian Analysis 4:1–30.

Clark, J. S., and S. L. LaDeau. 2006. Synthesizing ecological experiments and observational data with hierarchical Bayes. Pages 41–58 *in* J. S. Clark and A. Gelfand, editors. Hierarchical models of the environment. Oxford University Press, Oxford, UK.

Clark, J. S., S. LaDeau, and I. Ibáñez. 2004. Fecundity of trees and the colonization–competition hypothesis. Ecological Monographs 74:415–442.

Clark, J. S., E. Macklin, and L. Wood. 1998. Stages and spatial scales of recruitment limitation in southern Appalachian forests. Ecological Monographs 68:213–235.

Clark, J. S., M. Silman, R. Kern, E. Macklin, and J. Hille Ris Lambers. 1999. Seed dispersal near and far: generalized patterns across temperate and tropical forests. Ecology 80: 1475–1494.

Clark, J. S., M. Wolosin, M. Dietze, I. Ibáñez, S. LaDeau, M. Welsh, and B. Kloeppel. 2007*b*. Tree growth inferences and prediction from diameter censuses and ring widths. Ecological Applications 17:1942–1953.

Cole, W. G., and C. G. Lorimer. 2005. Probabilities of small-gap capture by sugar maple saplings based on height and crown growth data from felled trees. Canadian Journal of Forest Research 35:643–655.

Condit, R., et al. 2006. The importance of demographic niches to tree diversity. Science 313:98–101.

Connell, J. H. 1971. On the role of natural enemies in preventing competitive exclusion in some marine animals and in rain forest trees. Pages 298–312 *in* P. J. Boer and G. R. Graadwell, editors. Dynamics of numbers in populations. Centre for Agricultural Publishing and Documentation, Wageningen, The Netherlands.

Connell, J. H., and R. O. Slatyer. 1977. Mechanisms of succession in natural communities and their role in community stability and organization. American Naturalist 111: 1119–1144.

Craigmile, P. F., C. A. Calder, H. Li, R. Paul, and N. Cressie. 2009. Hierarchical model building, fitting, and checking: a behind-the-scenes look at a Bayesian analysis of arsenic exposure pathways. Bayesian Analysis 4:1–36.

Cressie, N., C. A. Calder, J. S. Clark, J. M. Ver Hoef, and C. K. Wikle. 2009. Accounting for uncertainty in ecological analysis: the strengths and limitations of hierarchical statistical modeling. Ecological Applications 19:553–570.

Dalling, J. W., and S. P. Hubbell. 2002. Seed size, growth rate and gap microsite conditions as determinants of recruitment success for pioneer species. Journal of Ecology 90:557–568.

Denslow, J. S. 1980. Gap partitioning among tropical rain forest trees. Biotropica 12(Supplement):47–55.

Denslow, J. S. 1987. Tropical rainforest gaps and tree species diversity. Annual Review of Ecology and Systematics 18: 431–451.

Dietze, M., and J. S. Clark. 2008. Changing the gap dynamics paradigm: Vegetative regeneration control on forest response to disturbance. Ecological Monographs 78:331–347.

Doblhammer, G., and J. Oeppen. 2003. Reproduction and longevity among the British peerage: the effect of frailty and health selection. Proceedings of the Royal Society B 270: 1541–1547.

Dribe, M. 2004. Long-term effects of childbearing on mortality: evidence from pre-industrial Sweden. Population Studies 58: 297–310.

Dunne, J. A., R. J. Williams, and N. D. Martinez. 2002. Network structure and biodiversity loss in food webs: robustness increases with connectance. Ecology Letters 5: 558–567.

Dunson, D. B. 2009. Comment on article by Craigmile et al. Bayesian Analysis 4:41–44.

Ellner, S. 1987. Alternate plant life history strategies and coexistence in randomly fluctuating environments. Vegetatio 69:199–208.

Engelbrecht, B. M. J., L. S. Comita, R. Condit, T. A. Kursar, M. T. Tyree, B. L. Turner, and S. P. Hubbell. 2007. Drought sensitivity shapes species distribution patterns in tropical forests. Nature 447:80–82.

Feeley, K. J., and J. W. Terborgh. 2008. Trophic drivers of species loss from fragments. Animal Conservation 11:366–368.

Geber, M. A. 1990. The cost of meristem limitation in *Polygonum arenastrum*: negative genetic correlations between fecundity and growth. Evolution 44:799–819.

Gel, Y., A. E. Raftery, and T. Gneiting. 2004. Calibrated probabilistic mesoscale weather field forecasting. Journal of the American Statistical Association 99:575–583.

Gelfand, A. E., and S. K. Ghosh. 1998. Model choice: a minimum posterior predictive loss approach. Biometrika 85: 1–11.

Gelman, A., and J. Hill. 2007. Data analysis using regression and multilevel/hierarchical models. Cambridge University Press, Cambridge, UK.

Geweke, J. F. 2004. Getting it right: joint distribution tests of posterior simulators. Journal of the American Statistical Association 99:799–804.

Gilbert, B., S. J. Wright, H. C. Muller-Landau, K. Kitajima, and A. Hernandez. 2006. Life history trade-offs in tropical trees and lianas. Ecology 87:1281–1288.

Gravel, D., C. D. Canham, M. Beaudet, and C. Messier. 2006. Reconciling niche and neutrality: the continuum hypothesis. Ecology Letters 9:399–409.

Grover, J. P. 1994. Assembly rules for communities of nutrient-limited plants and specialist herbivores. American Naturalist 143:258–282.

Grubb, P. J. 1977. The maintenance of species-richness in plant communities: the importance of the regeneration niche. Biological Reviews 52:107–145.

Gurevitch, J., and L. V. Hedges. 1999. Statistical issues in conducting ecological meta-analyses. Ecology 80:1142–1149.

Harms, K. E., S. J. Wright, O. Calderón, A. Hernández, and E. A. Herre. 2000. Pervasive density-dependent recruitment enhances seedling diversity in a tropical forest. Nature 404: 493–495.

Harper, J. L. 1977. Population biology of plants. Academic Press, London, UK.

Hastings, A. 1980. Disturbance, coexistence, history, and competition for space. Theoretical Population Biology 18: 363–373.

Hubbell, S. P. 2001. The unified neutral theory of biodiversity and biogeography. Princeton University Press, Princeton, New Jersey, USA.

Huisman, J., and F. J. Weissing. 1999. Biodiversity of plankton by species oscillations and chaos. Nature 402:407–410.

Hurt, L. S., C. Ronsmans, and S. L. Thomas. 2006. The effect of number of births on women's mortality: systematic review of the evidence for women who have completed their childbearing. Population Studies 60:55–71.

Hurtt, G. C., and S. W. Pacala. 1995. The consequences of recruitment limitation: reconciling chance, history and competitive differences between plants. Journal of Theoretical Biology 176:1–12.

Huston, M. A., and D. L. DeAngelis. 1994. Competition and coexistence: the effects of resource transport and supply rates. American Naturalist 144:954–977.

Huston, M. A., and T. M. Smith. 1987. Plant succession: life history and competition. American Naturalist 130:168–198.
Hutchinson, G. E. 1961. The paradox of the plankton. American Naturalist 95:137–145.
Ibáñez, I., J. S. Clark, and M. Dietze. 2008. Evaluating the sources of potential migrant species: implications under climate change. Ecological Applications 18:1664–1678.
Ibáñez, I., J. S. Clark, and M. Dietze. 2009. Estimating performance of potential migrant species. Global Change Biology 15:1173–1188.
Ibáñez, I., J. S. Clark, M. C. Dietze, K. Feeley, M. Hersh, S. LaDeau, A. McBride, N. E. Welch, and M. S. Wolosin. 2006. Predicting biodiversity change: outside the climate envelope, beyond the species–area curve. Ecology 87:1896–1906.
Ibáñez, I., J. S. Clark, S. LaDeau, and J. Hille Ris Lambers. 2007. Exploiting temporal variability to understand tree recruitment response to climate change. Ecological Monographs 77:163–177.
Inouye, R. S., and D. Tilman. 1988. Convergence and divergence of old-field plant communities along experimental nitrogen gradients. Ecology 69:995–1004.
Janzen, D. H. 1970. Herbivores and the number of tree species in tropical forests. American Naturalist 104:501–527.
Jobbágy, E. G., and R. B. Jackson. 2004. The uplift of soil nutrients by plants: biogeochemical consequences across scales. Ecology 85:2380–2389.
Kitajima, K. 1994. Relative importance of photosynthetic traits and allocation patterns as correlates of seedling shade tolerance of 13 tropical trees. Oecologia 98:419–428.
Kneitel, J. M., and J. M. Chase. 2004. Trade-offs in community ecology: linking spatial scales and species coexistence. Ecology Letters 7:69–80.
Kobe, R. K. 1996. Intraspecific variation in sapling mortality and growth predicts geographic variation in forest composition. Ecological Monographs 66:181–201.
Kohyama, T. 1993. Size-structured tree populations in gap-dynamic forest: the forest architecture hypothesis for the stable coexistence of species. Journal of Ecology 81:131–143.
Kramer, G. H. 1983. The ecological fallacy revisited: aggregated- versus individual-level findings on economics and elections, and sociotropic voting. American Political Science Review 77:92–111.
LaDeau, S., and J. S. Clark. 2001. Rising CO_2 and the fecundity of forest trees. Science 292:95–98.
LaDeau, S. L., and J. S. Clark. 2006. Elevated CO_2 and tree fecundity: the role of tree size, interannual variability, and population heterogeneity. Global Change Biology 12:822–833.
Latimer, A. M., S. Wu, A. E. Gelfand, and J. A. Silander, Jr. 2006. Building statistical models to analyze species distributions. Ecological Applications 16:33–50.
Levin, S. A. 1970. Community equilibria and stability, and an extension of the competitive exclusion principle. American Naturalist 104:413–423.
Levin, S. A. 1998. Ecosystems and the biosphere as complex adaptive systems. Ecosystems 1:431–436.
Levins, R. 1979. Coexistence in a variable environment. American Naturalist 114:765–783.
Lichstein, J. W., J. Dushoff, S. A. Levin, and S. W. Pacala. 2007. Intraspecific variation and species coexistence. American Naturalist 170:807–818.
Link, W. A., and R. J. Barker. 2006. Model weights and the foundations of multimodel inference. Ecology 87:2626–2635.
Loehle, C. 1987. Tree life history strategies: the role of defenses. Canadian Journal of Forest Research 18:209–222.
MacArthur, R. H. 1958. Population ecology of some warblers of northeastern coniferous forests. Ecology 39:599–619.
MacArthur, R. H., and R. Levins. 1964. Competition, habitat selection, and character displacement in a patchy environment. Proceedings of the National Academy of Sciences USA 51:1207–1210.
MacArthur, R., and R. Levins. 1967. The limiting similarity, convergence, and divergence of coexisting species. American Naturalist 101:377–385.
Mair, W., P. Goymer, S. D. Pletcher, and L. Partridge. 2003. Demography of dietary restriction and death in *Drosophila*. Science 301:1731–1733.
Mangel, M., and J. Stamps. 2001. Trade-offs between growth and mortality and the maintenance of individual variation in growth. Evolutionary Ecology 3:583–593.
Marks, C. O., and M. J. Lechowicz. 2006. Alternative designs and the evolution of functional diversity. American Naturalist 167:55–67.
McCarthy, B. C., and J. A. Quinn. 1992. Fruit maturation patterns of *Carya* spp. (Juglandaceae): an intra-crown analysis of growth and reproduction. Oecologica 91:30–38.
Meszéna, G., M. Gyllenberg, L. Pásztor, and J. A. J. Metz. 2006. Competitive exclusion and limiting similarity: a unified theory. Theoretical Population Biology 69:68–87.
Metcalf, C. J. E., J. S. Clark, and D. A. Clark. 2009*a*. Tree growth inference and prediction when the point of measurement changes: modelling around buttresses in tropical forests. Journal of Tropical Ecology 25:1–12.
Metcalf, C. J. E., J. S. Clark, and S. M. McMahon. 2009*b*. Overcoming data sparseness and parametric constraints in modeling of tree mortality: a new non-parametric Bayesian model. Canadian Journal of Forest Research 39:1677–1687.
Metcalf, C. J. E., M. Rees, J. M. Alexander, and K. E. Rose. 2006. Growth–survival trade-offs and allometries in rosette-forming perennials. Functional Ecology 20:217–225.
Mitton, J. B., and K. L. Duran. 2004. Genetic variation in piñon pine, *Pinus edulis*, associated with summer precipitation. Molecular Ecology 13:1259–1264.
Mohan, J. E., J. S. Clark, and W. H. Schlesinger. 2007. Long-term CO_2 enrichment of an intact forest ecosystem: implications for temperate forest regeneration and succession. Ecological Applications 17:1198–1212.
Myers, J. A., and K. Kitajima. 2007. Carbohydrate storage enhances seedling shade and stress tolerance in a neotropical forest. Journal of Ecology 95:383–395.
Natarajan, R., and R. E. McCulloch. 1998. Gibbs sampling with diffuse proper priors: a valid approach to data-driven inference? Journal of Computational and Graphical Statistics 7:267–277.
Naumburg, E., and D. S. Ellsworth. 2000. Photosynthesis sunfleck utilization potential of understory saplings growing under elevated CO_2 in FACE. Oecologia 122:163–174.
Obeso, J. R. 2002. The costs of reproduction in plants. New Phytologist 155:321–348.
Ogle, K. 2009. Hierarchical Bayesian statistics: Merging experimental and modeling approaches in ecology. Ecological Applications 19:577–581.
O'Hagan, A., and M. West. 2010. Handbook of Bayesian analysis. Oxford University Press, Oxford, UK.
Oren, R., J. S. Sperry, G. G. Katul, D. E. Pataki, B. E. Ewers, N. Phillips, and K. V. R. Schäfer. 1999. Survey and synthesis of intra- and interspecific variation in stomatal sensitivity to vapour pressure deficit. Plant, Cell and Environment 22: 1515–1526.
Pacala, S. W., C. D. Canham, J. Saponara, J. A. Silander, Jr., R. E. Kobe, and E. Ribbens. 1996. Forest models defined by field measurements. II. Estimation, error analysis, and dynamics. Ecological Monographs 66:1–43.
Pacala, S. W., and M. J. Crawley. 1992. Herbivores and plant diversity. American Naturalist 140:243–260.
Pacala, S. W., and D. Tilman. 1994. Limiting similarity in mechanistic and spatial models of plant competition in heterogeneous environments. American Naturalist 143:222–257.
Papiak, M. J., and C. D. Canham. 2006. Tree competition along environmental gradients in southern New England

forests: an application of multi-model inference. Ecological Applications 16:1880–1892.
Pascual, M. 2005. Computational ecology: from the complex to the simple and back. PLoS Biology 1:e18.
Pastor, J., J. D. Aber, C. A. McClaugherty, and J. M. Melillo. 1984. Above-ground production and N and P cycling along a nitrogen mineralization gradient on Blackhawk Island, Wisconsin. Ecology 65:256–268.
Peters, J., and K. Mengersen. 2008. Selective reporting of adjusted estimates in observational epidemiology studies: reasons and implications for meta-analyses. Evaluation and the Health Professions 31:370–389.
Pickett, S. T. A. 1989. Space-for-time substitution as an alternative to long-term studies. Pages 110–135 *in* G. E. Likens, editor. Long-term studies in ecology: approaches and alternatives. Springer-Verlag, New York, New York, USA.
Platt, W. J., G. W. Evans, and S. L. Rathbun. 1988. The population dynamics of a long-lived conifer (*Pinus palustris*). American Naturalist 131:491–525.
Poulson, T. L., and W. J. Platt. 1989. Gap light regimes influence canopy tree diversity. Ecology 70:553–555.
Primack, R., and E. Stacy. 1998. Cost of reproduction in the pink lady's slipper orchid (*Cypripedium acaule*, Orchidaceae): an eleven-year experimental study of three populations. American Journal of Botany 85:1672–1679.
Rees, M., R. Condit, M. Crawley, S. Pacala, and D. Tilman. 2001. Long-term studies of vegetation dynamics. Science 293: 650–655.
Reich, P. B., M. B. Walters, and D. S. Ellsworth. 1997. From tropics to tundra: Global convergence in plant functioning. Proceedings of the National Academy of Sciences USA 94: 13730–13734.
Reznik, D. 1985. Costs of reproduction: an evaluation of the empirical evidence. Oikos 44:257–267.
Ricklefs, R. E., and C. D. Cadena. 2007. Lifespan is unrelated to investment in reproduction in populations of mammals and birds in captivity. Ecology Letters 10:867–872.
Royle, J. A., and R. M. Dorazio. 2008. Hierarchical modeling and inference in ecology: the analysis of data from populations, metapopulations and communities. Academic Press, San Diego, California, USA.
Russo, S. E., P. Brown, S. Tan, and S. J. Davies. 2008. Interspecific demographic trade-offs and soil-related habitat associations of tree species along resource gradients. Journal of Ecology 96:192–203.
Scott, J. G., and J. O. Berger. *In press*. Bayes and empirical-Bayes multiplicity adjustment in the variable-selection problem. Annals of Statistics.
Sharp, W. M., and V. G. Sprague. 1967. Flowering and fruiting in the white oaks. Pistillate flowering, acorn development, weather, and yields. Ecology 48:243–251.
Silman, M. R. 2006. Plant species diversity in Amazonian forests. Pages 269–294 *in* M. Bush and J. Flenly, editors. Tropical rain forest responses to climate change. Praxis Publishing, Springer-Praxis, London, UK.
Silvertown, J. 2004. Plant coexistence and the niche. Trends in Ecology and Evolution 19:605–611.
Silvertown, J., and M. Dodd. 1999. The demographic cost of reproduction and its consequences in balsam fir (*Abies balsamea*). American Naturalist 154:321–332.
Silvertown, J., M. Franco, I. Pisanty, and A. Mendoza. 1993. Comparative plant demography: relative importance of life-cycle components to the finite rate of increase in woody and herbaceous perennials. Journal of Ecology 81:465–476.
Sipe, T. W., and F. A. Bazzaz. 1995. Gap partitioning among maples (*Acer*) in central New England. Ecology 76:1587–1602.
Spiegelhalter, D. J., N. G. Best, B. P. Carlin, and A. van der Linde. 2002. Bayesian measures of model complexity and fit. Journal of the Royal Statistical Society Series B 64:583–639.
Tatar, M., and J. R. Carey. 1995. Nutrition mediates reproductive trade-offs with age-specific mortality in the beetle *Callosobruchus*. Ecology 76:2066–2073.
Thomas, S. C. 1996. Relative size at the onset of maturity in rain forest trees: a comparative analysis of 37 Malaysian species. Oikos 76:145–154.
Tilman, D. 1982. Resource competition and community structure. Monographs in population biology 17. Princeton University Press, Princeton, New Jersey, USA.
Tilman, D. 1985. The resource-ratio hypothesis of plant succession. American Naturalist 125:827–852.
Tilman, D. 1988. Dynamics and structure of plant communities. Monographs in population biology 26. Princeton University Press, Princeton, New Jersey, USA.
Tilman, D. 1994. Competition and biodiversity in spatially structured habitats. Ecology 75:2–16.
Tilman, D. 2004. Niche tradeoffs, neutrality, and community structure: a stochastic theory of resource competition, invasion, and community assembly. Proceedings of the National Academy of Sciences USA 101:10854–10861.
Uriarte, M., C. D. Canham, J. Thompson, and J. K. Zimmerman. 2004. A neighborhood analysis of tree growth and survival in a hurricane-driven tropical forest. Ecological Monographs 74:591–614.
Valladares, F., and Ü. Niinemets. 2008. Shade tolerance, a key plant feature of complex nature and consequences. Annual Review of Ecology, Evolution, and Systematics 39:237–257.
Vaupel, J. W., K. G. Manton, and E. Stallard. 1979. The impact of heterogeneity in individual frailty on the dynamics of mortality. Demography 16:439–454.
Ver Hoef, J. M., and K. Frost. 2003. A Bayesian hierarchical model for monitoring harbor seal changes in Prince William Sound, Alaska. Environmental and Ecological Statistics 10: 201–209.
Vieilledent, G., B. Courbaud, G. Kunstler, J.-F. Dhôte, and J. S. Clark. 2009. Biases in the estimation of size dependent mortality models: advantages of a semi-parametric approach. Canadian Journal of Forest Research 39:1430–1443.
Volkov, I., J. R. Banavar, S. P. Hubbell, and A. Marutan. 2003. Neutral theory and relative species abundance in ecology. Nature 424:1035–1037.
Walters, M. B., and P. B. Reich. 1996. Are shade tolerance, survival, and growth linked? Low light and, nitrogen effects on hardwood seedlings. Ecology 77:841–853.
Weiner, J., P. Stoll, H. Muller-Landau, and A. Jasentuliyana. 2001. The effects of density, spatial pattern and competitive symmetry on size variation in simulated plant populations. American Naturalist 158:438–450.
Welden, C. W., S. W. Hewett, S. P. Hubbell, and R. B. Foster. 1991. Sapling survival, growth, and recruitment: relationship to canopy height in a neotropical forest. Ecology 72:35–50.
Wikle, C. K. 2003. Hierarchical Bayesian models for predicting the spread of ecological processes. Ecology 84:1382–1394.
Wikle, C. K., and L. M. Berliner. 2005. Combining information across spatial scales. Technometrics 47:80–91.
Wright, I. J., et al. 2004. The worldwide leaf economics spectrum. Nature 428:821–827.
Wright, S. J. 2002. Plant diversity in tropical forests: a review of mechanisms of species coexistence. Oecologia 130:1–14.
Würth, M. K. R., S. Peláez-Riedl, S. J. Wright, and C. Körner. 2005. Non-structural carbohydrate pools in a tropical forest. Oecologia 143:11–24.
Wyckoff, P. H., and J. S. Clark. 2000. Predicting tree mortality from diameter growth: a comparison of maximum likelihood and Bayesian approaches. Canadian Journal of Forest Research 30:156–167.
Wyckoff, P. H., and J. S. Clark. 2002. Growth and mortality for seven co-occurring tree species in the southern Appalachian Mountains: implications for future forest composition. Journal of Ecology 90:604–615.

Wyckoff, P., and J. S. Clark. 2005. Comparing predictors of tree growth: the case for exposed canopy area. Canadian Journal of Forest Research 35:13–20.
Yoda, K., K. Shinozaki, H. Ogawa, K. Hozumi, and T. Kira. 1965. Estimation of total amount of respiration from woody organs of trees and forest communities. Journal of Biology 16:15–26.
Zillio, T., and R. Condit. 2007. The impact of neutrality, niche differentiation and species input on diversity and abundance distributions. Oikos 116:931–940.

APPENDIX A

Prior distributions, conditional relationships and distribution theory needed for algorithm development, algorithms used for Metropolis within Gibbs, and some issues related to MCMC diagnostics (*Ecological Archives* M080-020-A1).

APPENDIX B

Parameter estimates, by species (*Ecological Archives* M080-020-A2).